STUDY OF DELAY CALCULATION FOR DIVERGING DIAMOND INTERCHANGE AND SAFETY ASSESSMENT OF ECODRIVING ON FOLLOWING TRAFFIC

Xi Duan

Thesis submitted to the faculty of the Virginia Polytechnic Institute and State University
in partial fulfillment of the requirements for the degree of

Master of Science
In
Civil Engineering

Montasir Abbas, Chair
Antonio A. Trani
Gerardo W. Flintsch

May 5th, 2017
Blacksburg, VA

Keywords: Delay, diverging diamond interchange, ecodriving, safety

STUDY OF DELAY CALCULATION FOR DIVERGING DIAMOND INTERCHANGE AND SAFETY ASSESSMENT OF ECODRIVING ON FOLLOWING TRAFFIC

Xi Duan

ABSTRACT

Diverging diamond interchanges (DDI) have been proved to outperform other types of diamond interchanges in terms of safety, cost-effectiveness and efficiency, but few research efforts have been done to conduct the analytic calculation of delay, with which optimization of timing plans can be acquired more efficiently. This paper develops the control strategies based on the introduction of overlap and offset analysis, which provide a uniform representation of sequences for DDI signal control. Based on the developed timing plan then the delay calculation equations are put forward and results show the calculation fit simulation very well with R-Square to be 0.9949 for total delay of those two directions

Ecodriving aims to achieve the best fuel efficiency by guiding vehicles travel at planned and optimized speed trajectories. This study opens the door for safety concerns for following normal driving vehicles (FNVs) when following ecodriving vehicles (EVs). To examine the safety issues under different circumstance. Three road elements: initial signal status, ambient vehicles and speed limit along with three EV elements: SpeedTolimit, DistanceToStoplight and acceleration were chosen as potential influential elements, and time to collision (TTC) was selected as the dependent variable. Therefore, six testing

scenarios and six baseline were designed and implemented using a drive safety DNS-250 simulator. 29 drivers participated in the driving simulator study. The results show the aforementioned road elements and EV elements have significant influence on TTC of FNV in different testing parts. Therefore, these finding can be used as guidance for future ecodriving algorithm design and implementation.

STUDY OF DELAY CALCULATION FOR DIVERGING DIAMOND INTERCHANGE AND SAFETY ASSESSMENT OF ECODRIVING ON FOLLOWING TRAFFIC

Xi Duan

GENERAL AUDIENCE ABSTRACT

The research conducted in the thesis are composed of two sub-topics: delay calculation for diverging diamond interchange and safety assessment of ecodriving, on following traffic. Both of them are new coming technologies and are attracting increasing research interests. The first research topic, diverging diamond interchange is a new design of interchange which aims to decrease the conflict points of intersection hence increase the safety and efficiency. The second topic is about ecodriving, which is a vehicles communication-related topic, aims to improve fuel efficiency by taking better use of signal phasing and timing (SPaT) information. Both of them will contribute to the construction of environment-friendly and safe transportation systems. The research on these topic are innovative and should play role in guiding follow-up research in the future.

ACKNOWLEDGEMENTS

I would like to thank my parents for supporting me to accomplish my master degree, both financially and spiritly. They make me be free of financial problems so I can fully concentrate on my study and research.

Besides, I want to show my gratitude to my advisor Dr. Montasir Abbas, I really appreciate his guidance and help in my study and research. Dr. Abbas's sense of humor and enthusiasm bring courage and inspiration to me. I also want to thank my committee member Dr. Antonio A. Trani and Dr. Gerardo W. Flintsch for their helpful lecture and helps with the accomplishment of my master degree.

Additionally, I would like to thank Dr. Antoine G. Hobeika, Dr. Hesham A. Rakha and Dr. Pamela Murray-Tuite for their amazing lecture. They are always respectful and patient for every student

Moreover, I want to extend my appreciation to my friends in Virginia Tech ITSE program, thank for accompanying me and helping me with my simulator driving test.

ATTRIBUTIONS

Dr. Montasir Abbas is the supervisor in guiding me to finish the research shown in chapter 4 and chapter 5. Dr.Abbas provided me with suggestions on determining the feasible topic, conducting experimental designs and doing analysis.

The chapter 4 of the thesis was presented in IEEE 19th International Conference on ITSC, 2016, and was published in the conference proceedings.

The chapter 5 of the thesis was submitted to IEEE 20th International Conference on ITSC, 2017.

LIST OF CONTENTS

ABSTRACT ..... **ii**

GENERAL AUDIENCE ABSTRACT ..... **iv**

ACKNOWLEDGEMENTS ..... **v**

ATTRIBUTIONS ..... **vi**

LIST OF CONTENTS ..... **vii**

LIST OF FIGURES ..... **ix**

LIST OF TABLES ..... **xi**

CHAPTER 1 INTRODUCTION **1**

CHAPTER 2 LITERATURE REVIEW **2**

CHAPTER 3 MACROSCOPIC CALCULATION OF DELAY FOR DIVERGING DIAMOND INTERCHANGES **6**

3.1 ABSTRACT 7

3.2 INTRODUCTION 8

3.3 FEATURE ANALYSIS 8

3.3.1 Sequence and Overlap 9

3.3.2 Offset 11

3.4 DELAY CALCULATION 12

3.4.1 Difference on Delay Calculation of DDI 12

3.4.2 Delay Calculation of Westbound Internal Lane 16

3.4.3 Delay Calculation of Eastbound Internal Lane 20
3.5 SIMULATION AND VERIFICATION 21
CHAPTER 4 SAFETY ASSESSMENT OF ECODRIVING VEHICLES ON FOLLOWING TRAFFIC 25
4.1 ABSTRACT 26
4.2 INTRODUCTION 27
4.3 ECODRIVING ALGORITHM 28
4.4 EXPERIMENTAL DESIGN 32
4.4.1 Purpose of the Experiments 32
4.4.2 Road and EV Elements Considered 33
4.4.3 Implementation 35
4.5 ANALYSIS AND RESULTS 40
4.5.1 Pretreatment For Time To Collision 40
4.5.2 Examination Of Road Elements 40
4.5.3 Check The Interaction Between Initial Signal Statuses With EV Elements. 42
4.5.4 Comparisons With Baseline 43
4.5.5 Examination For EV Elements 48
4.6 FUTURE RESEARCH 50
CHAPTER 5 SUMMARY OF CONCLUSION AND FUTURE RESEARCH 52
REFERENCE 56

LIST OF FIGURES

FIGURE 3-1 LAYOUT OF SIGN 9

FIGURE 3-2 BASIC SEQUENCE 10

FIGURE 3-3 LAYOUT OF CONFLICT POINTS, MERGE POINTS AND INFLOW, OUTFLOW LANE CONCERNED 10

FIGURE 3-4 TWO TYPE OF SEQUENCE OF DDI. 11

FIGURE 3-5 DIFFERENT SEQUENCES, (A) IS SEQUENCE 1 AND (B) IS SEQUENCE 2. 12

FIGURE 3-6 BASIC CUMULATIVE VEHICLE-TIME DIAGRAM 12

FIGURE 3-7 DIFFERENT ARRIVAL PATTERNS 14

FIGURE 3-8 DIFFERENT INFLUENCE OF OFFSET AND TRAVEL TIME ON WESTBOUND AND EASTBOUND INTERNAL LANE, (A) IS EASTBOUND, (B) IS WESTBOUND 15

FIGURE 3-9 DELAY CALCULATION DIAGRAM 18

FIGURE 3-10 FLOW CHART OF CALCULATION LOGIC 21

FIGURE 3-11 COMPARISON FOR WESTBOUND INTERNAL LANE 23

FIGURE 3-12 COMPARISON FOR EASTBOUND INTERNAL LANE 23

FIGURE 3-13 COMPARISON OF TOTAL DELAY OF THOSE TWO DIRECTIONS 24

FIGURE 4-1 OPTIMIZATION HORIZON LAYOUT 29

FIGURE 4-2 COMPONENTS VEHICLES 35

FIGURE 4-3 PARAMETERS SETTING 37

FIGURE 4-4 SPEED TRAJECTORIES (A) IS ECODRIVING (B) IS NORMAL-DRIVING 38

FIGURE 4-5 DRIVE-SAFETY DS-250 38

FIGURE 4-6 LAYOUT OF SIMULATION NETWORK 39

FIGURE 4-7 INITIAL SIGNAL PART 1 44
FIGURE 4-8 DECELERATION PART 44
FIGURE 4-9 INITIAL ACCELERATION PART 45
FIGURE 4-10 ACCELERATION PART 45
FIGURE 4-11 WHOLE OPTIMIZATION HORIZON 45

LIST OF TABLES

TABLE 3-1 CONFLICT, MERGE AND DIVERGE RELATIONSHIP BETWEEN SIGNAL GROUPS 9

TABLE 3-2 CONFLICT AND MERGE POINTS CONCERNED 10

TABLE 3-3 INPUT VARIABLE FOR JMP 22

TABLE 3-4 . R-SQUARE OF RESULTS 24

TABLE 4-1 ROAD ELEMENTS TYPES AND LEVELS 33

TABLE 4-2 SCENARIOS DESIGN 35

TABLE 4-3 RESULTS OF VARIANCE ANALYSIS 41

TABLE 4-4 COMPARISONS BETWEEN DIFFERENT SPEED LIMIT 42

TABLE 4-5 COEFFICIENTS OF REGRESSION 43

TABLE 4-6 MODEL SUMMARY 43

TABLE 4-7 RATE OF CRITICAL SECONDS FOR PARTS WITH DIFFERENT INITIAL SIGNAL STATUS 47

TABLE 4-8 RATES OF DIFFERENT TTC VALUE RANGE FOR PARTS WITH DIFFERENT INITIAL SIGNAL STATUS 47

TABLE 4-9 RATES OF CRITICAL SECONDS FOR PARTS WITH DIFFERENT SPEED LIMIT 47

TABLE 4-10 RATES OF DIFFERENT TTC VALUE RANGE FOR PART WITH DIFFERENT SPEED LIMIT 48

TABLE 4-11 COEFFICIENTS OF REGRESSION FOR DECELERATION PART 48

TABLE 4-12 MODEL SUMMARY 49

TABLE 4-13 COEFFICIENTS OF REGRESSION FOR ACCELERATION PART 50

TABLE 4-14 AVERAGED ACCELERATION 50

CHAPTER 1 INTRODUCTION

The work presented in this thesis contain two manuscripts: the first paper is about macroscopic delay calculation for diverging diamond interchange. This research shows an innovative numerical delay calculation method for the internal lane of diverging diamond interchange, which can be applied for different configurations of diverging diamond interchange, 39 traffic pattern were examined through VISSIM simulation and high R square value shows the high accuracy of the delay calculation. The second paper did a safety assessment of ecodriving vehicles on following traffic. This study opens the door for safety concern for vehicles following ecodriving vehicles (EVs), three road elements and three ecodriving vehicles elements are considered, which then used for scenarios design which simulated in simulator with 29 drivers. The results show these road elements and EV elements have significant influence on the safety of following vehicles which indicated by time to collision value.

CHAPTER 2 LITERATURE REVIEW

In the U.S., the transportation sector accounted for around 73% of petroleum-based fuel consumption (including gasoline and diesel) in 2015 [1], which in turn corresponded to 26% GHG generation source [2]. Improving fuel efficiency not only helps drivers save money, but also plays important roles in reducing emission-related air pollution and relieving the world-wide climate warming.

Ecodriving is one the ways aim to improve fuel efficiency, which is achieved through mainly two ways. First, through providing general driving tips to the drivers, such as reducing high speed, driving smoothly, accelerating slowly, etc. A previous study assessed the effectiveness of static, web-based information on ecodriving with sample of 100 students, staff and faculties [3]. It found even small shifts in behavior attributable to inexpensive dissemination of information could be deemed cost-effective in reducing fuel consumption and emissions. Another research discovered that the ecodriving programs affected the driving performance of the drivers both on the training day and in the real-world driving cases significantly, and the programs not only improved the fuel economy values for drivers in developing region like Manila, but also these in developed district such as Tokyo [4].

Another application of ecodriving is to provide dynamic real-time advice to drivers or even operate on the vehicles (autonomous vehicles) directly to follow the planned and optimized speed trajectory in order to achieve the highest fuel efficiency [5-17], which requires higher technology level.

For the ecodriving algorithm development, most of the research set the objective to achieve the highest fuel efficiency hence obtain minimal emission, as they are firmly correlated. However, a study noticed the tradeoff between the achievement of the best fuel efficiency and the least travel time [6]. Therefore, it proposed an algorithm that is able to have a linear combination of travel time and fuel

consumption. Another reserach sought to achieve minimization of different types of emission by setting a different ecospeed limit and maximum throttle level for ecodriving vehicles (EVs) [7].

In respect of the research scope, some research focused their scope on rolling area [5]. In this study, an optimal controller for hybrid electric vehicles running on rolling terrain was developed. Others mainly concentrating on making better use of signal phasing and timing (SPaT) information of the signals in the urban areas [6-17]. A research tested the efficiency of eco-approach technology by running a car with cellular network link past a single intersection and simulating it in the software as well [8]. Other research developed an ecodriving control algorithm which guided ecodriving vehicles to adjust its speed to pass through several intersections in an arterial with high fuel efficiency[9, 10].

As for the constraints considered in the models, besides the SPaT of intersection, the downstream vehicles were incorporated as a constraint as well. Some studies involve the downstream vehicles by estimating the dissipating time of downstream platoon [6, 11]. Other research assumed that the eco-driving cars were able to predict the future status of the preceding vehicles with V2V technology, which will keep collecting the data include the location, speed and acceleration of leading vehicles [12]. A previous research adopted the safe distance between the following car and the leading car as a constraint, with which the following car should always keep [13]. Another study did further to take time inter vehicular (TIV), time to collision (TTC) into considerations, all these parameters were used to constrain the car-following behavior of ecodiving vehicles [14]. Other research incorporated both ecodriving speed trajectory and car-following behavior in their models, certain threshold such as spacing was set to switch from ecodriving to normal car-following behaviors [15-17]. Moreover, the topography information was also involved as a constraint in some research that targeted for optimization of signalized urban areas [13, 16, 17].

The effectiveness of ecodriving has been generally proved. However, there are several elements that can cause the variation of the effectiveness of eco-driving technologies. For human drivers, the knowledge level about ecodriving and the different characteristics of the drivers will make a difference [3, 4]. It was

discovered that the drivers who attended the ecodriving training program tend to have better fuel-efficiency driving performance which suggests that drivers could adapt well to ecodriving techniques in developing, as well as developed country settings [3]. The key characteristics of the drivers who found to have improved driving performance during experiments included being female, living in smaller households, and owning a newer car with higher fuel economy [4]. The types of equipment being used to convert advice to drivers also have impact on the performance of ecodriving [18, 19]. On board equipment proved to outperform variable message sign (VMS) [18]. It was found in this research that the roadside signaling system was not accurate and could confuse drivers while on-board speed recommendations could provide more accurate and dynamic information, which enable drivers easily focus and follow the speed advice. Drivers tend to have better ecodriving behavior with hybrid interface in the vehicle, but at the same time, it could cause distraction to drivers [20]. The benefit of visual, combined visual-auditory or haptic system for providing useful eco-driving advice to the driver regarding fuel efficient accelerator pedal usage were discussed. The strong force feedback system was recommended for further testing as it produced the strongest objective and subjective performance in terms of system effectiveness amongst the haptic systems in this study [19].

There are some other studies concerned autonomous vehicles, or vehicles with assumption that human factors could be excluded from the concerns by assuming drivers were able to follow the advice exactly. The priority weight between travel time and fuel efficiency set in the model was found have profound impact on the fuel efficiency performance [6]. A previous research proposed that greater energy savings (up to 8%) could be achieved without adversely affecting travel time if the arrival speed could be relaxed. [13]. Another study revealed that the effectiveness of ecodriving will be compromised with the increasing communication delay, while its effectiveness is more sensitive to the communication range, as wider range enable better performance [11]. A study found that the headway between leading and following vehicles and the intended behavior of them also works as influential factors [15]. It further concluded that a smaller headway resulted in less fuel consumption when the platoon needed to accelerate to pass the intersection, whereas a larger

headway leaded to less fuel consumption if the vehicles decelerate to pass through intersections. The grade of the road [13]and the hilly road density also play important roles in varing the performance of ecodriving [7]. Besides, another research found that the value of predefined constraint such as TTC which ensure the safe driving condition of ecodriving vehicles will make the improvement of ecodriving drop by 16–54% [14]. Some research stated that the different trip profile, including the number of intersections and total trip length, cause the variation of fuel savings from ecodriving in each trip[16]. Another research discovered that the penetration level, as well as the congestion level were two main factors impact the ecodriving performance. It concluded system-wide fuel and delay savings were not achieved when the market penetration level was less than 50% and higher savings were made at lower levels of traffic congestion [17].

Diamond interchanges were developed to connect the highway system with the local street system. In order to increase the capacity and decrease the delay of diamond interchange, new design have been put forward, among which Diverging diamond interchange (DDI) and Single-point urban interchanges (SPUI) are most practical. Lots of research was conducted to compare DDI, SPUI and Conventional diamond interchange (CDI). DDI was proved to outperform other type of diamond interchange in terms of safety, cost-effectiveness and efficiency [24], and DDI was found to be especially suitable for the scenarios when the heaviest movements are left- or right-turning movements onto or off the ramps. More specifically, three-phase configuration of timing plan of DDI is proven to outperform two phase timing control by increasing the movement on internal lane of DDI [25]. However, most of those research efforts were conducted based on simulation, even a research developed a model to calculate the control delay of movement on internal lane and external lane of DDI by taking spillback into consideration [26]. It fails to consider the factor that the arrival rate on internal lane will vary during the time which results from the upstream traffic control, which leads the model to be inaccurate and ineligible for coordination optimization.

CHAPTER 3 MACROSCOPIC CALCULATION OF DELAY FOR DIVERGING DIAMOND INTERCHANGES

Xi Duan
Charles Via Department of Civil and Environmental Engineering
301-D, Patton Hall
Virginia Polytechnic Institute and State University
Blacksburg, VA, 24061
E-mail: xiduan@vt.edu

Montasir M. Abbas, Ph.D., P.E. (Corresponding Author)
Associate Professor
Charles Via Department of Civil and Environmental Engineering
301-A, Patton Hall
Virginia Polytechnic Institute and State University
Blacksburg, VA, 24061
Phone: (540) 231-9002
E-mail: abbas@vt.edu

3.1 ABSTRACT

Diverging diamond interchanges (DDI) have been proved to outperform other types of diamond interchanges in terms of safety, cost-effectiveness and efficiency, but most of those research efforts were based on case studies using simulation or empirical analysis. Few research efforts have been done to conduct the analytic calculation of delay, with which optimization of timing plans can be acquired more efficiently. This paper first develops the control strategies based on the introduction of overlap and offset analysis, which provide a uniform representation of sequences for DDI signal control. Considering the difference of delay calculation between DDI and isolated intersections, as the inflows will serve either as saturated flow or arrival rate from either upstream ramp or arterial, delay equations were developed to calculate the delay on the internal lanes of DDI, which can be used for all different undersaturated traffic. Finally, 39 different traffic patterns that each with 10 decision variables created from JMP are used to check the accuracy of the calculations using VISSIM software. The results show the calculation fit simulation very well with R-Square to be 0.9968 for delay calculation of westbound internal lane, 0.9914 for eastbound internal lane, and 0.9949 for total delay of those two directions. By changing the pre-determined parameters such as the length of internal lanes, saturated flow rate of upstream approach, desired speed, all-red and amber time, the equations proposed in the paper are actually able to take all kinds of configurations of DDI into consideration and get the optimized timing plan easily with commercial solvers.

Keywords— DDI; delay; internal lane; timing plan; patterns

3.2 INTRODUCTION

In this study, timing plans are developed step by step based on ring barrier control (RBC). Using a scheme of overlaps and offsets, the different sequences of DDI is modeled with an uniform structure that can be easily analyzed and used for delay calculation and timing optimization. Secondly, the difference between the delay calculation of DDI and isolated intersection are analyzed, and the delay calculations of DDI for undersaturated traffic are proposed. Finally, VISSIM 7.0 was used to verify the accuracy of the analytical calculations by comparing the results from VISSIM output to the calculation results with 39 different input created from JMP. The proposed calculations show high accuracy and robustness with R-Square values of 0.9968 of delay calculation for westbound internal lane, 0.9914 for eastbound internal lane, and 0.9949 for total delay of those two directions.

3.3 FEATURE ANALYSIS

Guiding the two directions of traffic of the arterial to drive on the opposite side of the roadway on the bridge decreases the crossing conflict points of DDI to 2, with 8 merging points and 8 diverging points in total. For those traffic control which focus on the control strategies developed to control the movement of left- and right- turn from ramp, and through movement from arterial, there are 8 signal heads in total. However, considering DDI is most suitable for the situations in which heavy traffic flow are presented from left- or right- turn movement on or off the ramp, all 8 movements considered to be controlled by the signal as labeled in Fig. 3-1.

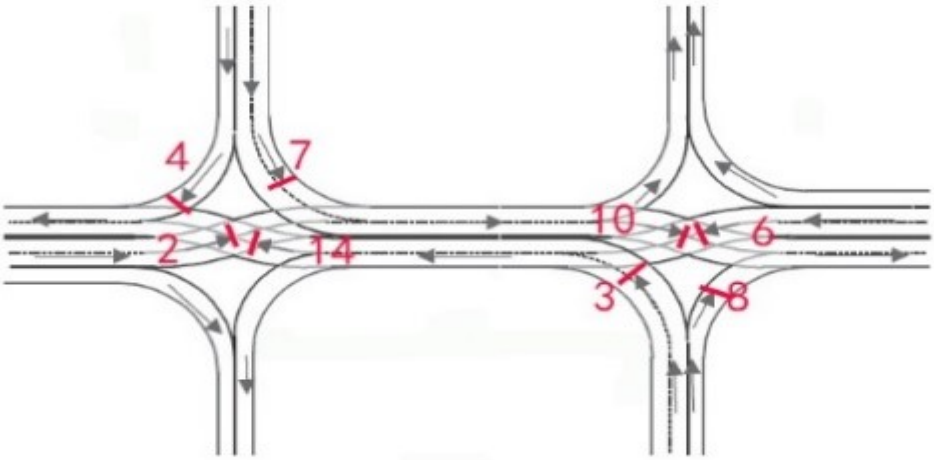

Figure 3-1 Layout of sign

The conflict, merge, diverge correlations among those 8 signal groups are also listed in Table 3-1 to help illustrate the features of DDI better.

Table 3-1 Conflict, merge and diverge relationship between signal groups

Type / Signal group	Conflict	Merge	Diverge
2	14	7	
3		6	8
4		14	7
6	10	3	
7		2	4
8		10	3
10	6	8	
14	2	4	

3.3.1 Sequence and Overlap

As shown in the table, signal groups are only in conflict or merge with those signal groups at the same sub-intersection, so ring 1 and ring 2 in a NEMA controller scheme are created to accommodate the signal at the same intersection as shown in Figure.3-2

4	7	2	14
10	6	3	8

Figure 3-2 Basic sequence

Those 8 signal groups are involved in 2 conflict points and 2 merge sections. These 2 conflict points and 2 merge sections which presented in the internal of intersection are critical for the development of control strategies, as shown in Figure 3-3, since they determine the inflow and outflow of DDI. Inflow is defined as the traffic flow that get into the intersection, which controlled by 3, 6, 7, 2 in this study, and outflow movements are controlled by 14 and 10, for another 2 merge sections. However, the right turn from ramp could pass only if the outflow turn red, so they are less important and are not given priority in developing overlaps.

Table 3-2 Conflict and merge points concerned

Classification	Inflow	outflow
Conflict 1	2	14
Conflict 2	6	10
Merge 1	7 2	
Merge 2	6 3	

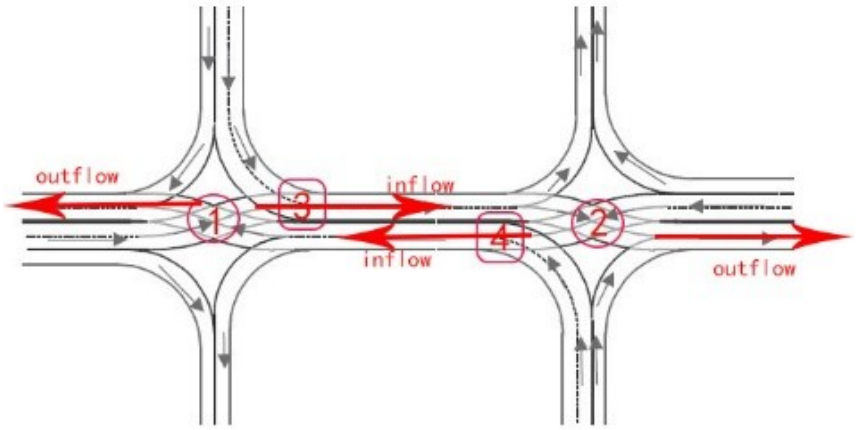

Figure 3-3 Layout of conflict points, merge points and inflow, outflow lane concerned

The control strategies should make better use of the inflow internal lanes, and outflow external lanes, which are shown in Table 3-2. Signal group 2 conflicts with 14 and

7, while signal group 6 conflicts with 3 and 10. So 14 and 7 are set to be overlapped as one signal group to achieve the most efficiency, and 3 and 10 are overlapped for the same reason. Since right turn movements only conflict with the outflow, signal group 4 and 8 are set to overlap with 2 and 6, resulting in two kind of sequences which are shown in Figure 3-4.

14 & 7	2 & 4
3 & 10	6 & 8

Sequence 1

14 & 7	2 & 4
6 & 8	3 & 10

Sequence 2

Figure 3-4 Two type of sequence of DDI.

3.3.2 **Offset**

The two sub-intersections of DDI are controlled by separate rings of RBC. By introducing an offset, a better timing plan can be made by coordinating those two intersections together.

An offset is define as the difference between phase 3&10 and 14&7, those two sequences in Figure 3-4 can be achieved by varying the offset from 0 to cycle length. In some studies, coordination is only conducted for arterials, which result in missing of optimized timing plan when critical flow served from ramps. However, with the proposed sequences that incorporate overlap and offset, both ramp and arterial traffic can be coordinated.

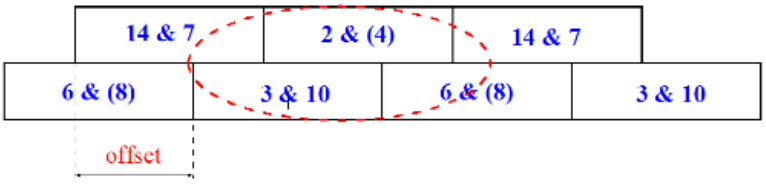

(a)

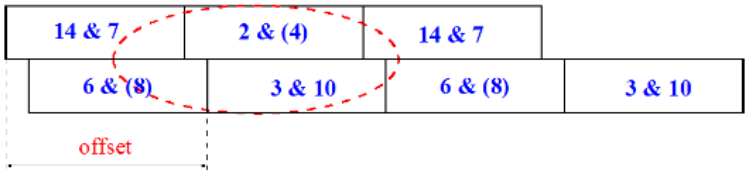

(b)

Figure 3-5 Different sequences, (a) is sequence 1 and (b) is sequence 2.

3.4 DELAY CALCULATION

3.4.1 Difference on Delay Calculation of DDI

The delay calculations proposed by HCM are based on the time-cumulative vehicle diagram, the method is able to calculate the delay of a certain section by counting the time difference between vehicles entering and leaving the section, minus the travel time of vehicles traveling through the section at free flow speed.

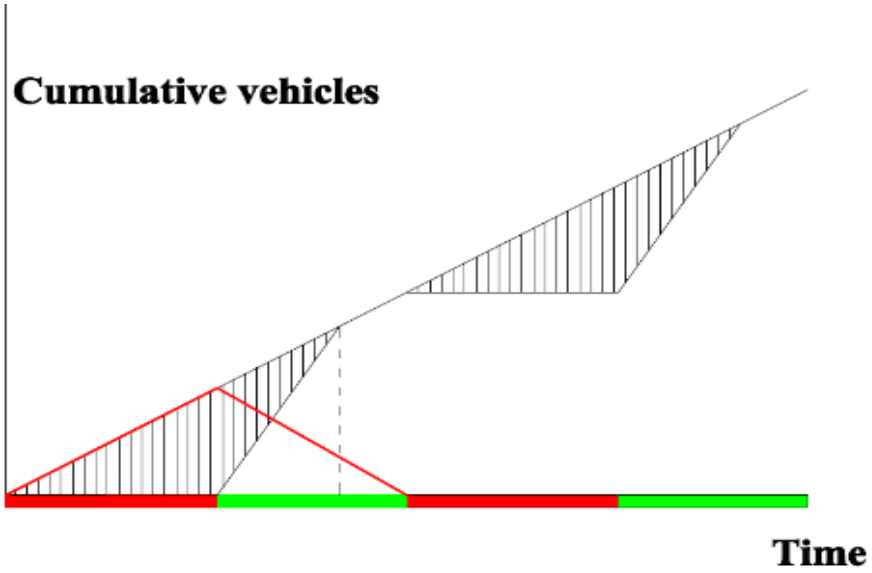

Figure 3-6 Basic cumulative vehicle-time diagram

In Figure 3-6, the curve above is the cumulative arrival curve, and the curve below represent the cumulative departure. The arrival curve has been shifted to the right with the value of travel time at free-flow. The area between those 2 curves represent the total delay when vehicles travel through the section instead of the total travel time. For delay calculation, the first method is to measure the area between cumulative arrival curve and cumulative departure curve directly, which is marked with shadows in Figure 3-6. The second method is to calculate the area of queuing curve which is marked as the red triangle shown in Figure 3-6.

Although the delay calculation proposed in this paper share a similar idea with the HCM, the delay calculation of DDI differ from isolated intersection in internal lanes. For isolated intersections, only a constant traffic flow from upstream is served as inflow. However, for the internal lane of DDI, the inflows are either from ramp or arterial, and are either served as saturated flow or only arrival rates. The different arrival patterns will lead to different delay, as shown in Figure 3-7. The figure shows: (a) arrival rate served first and (b) saturated flow served first. Different orders result in different total delay, even though they share the same total arrival in a cycle. It should also be noted that with different saturated flow rate and arrival rate from ramp and arterial, the variability increase even more.

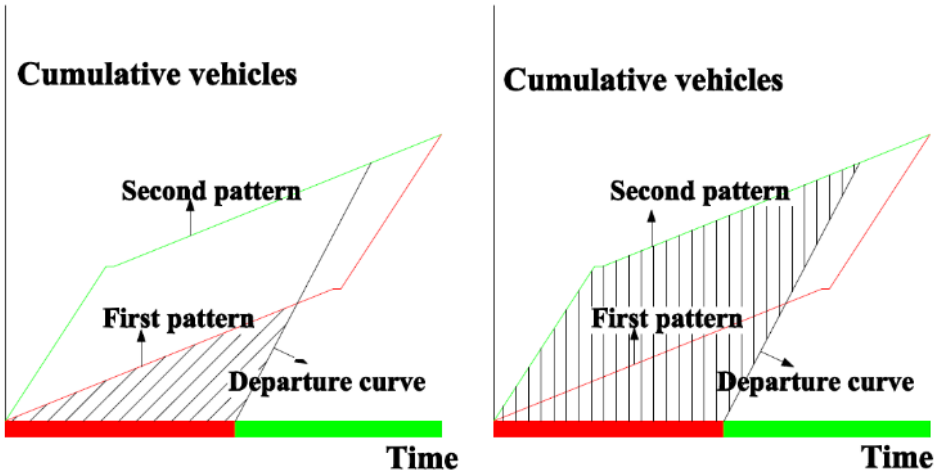

Figure 3-7 Different arrival patterns

In this study, internal lanes are controlled by signal group 14&7 (westbound) and 3&10 (eastbound). Take westbound traffic flow as example: the inflow of internal lane is either from left turn off ramp flow controlled by signal group 3&10, or through movement from arterial controlled by signal group 6&8. The traffic is either served as a saturated flow or arrival rate, depend on the signal control of upstream signal groups 3&10 and 6&8. The calculation therefore is complex and need to consider all phasing sequence possibilities.

(1)Difference of delay calculation between westbound and eastbound:

Generally, the westbound internal lanes and eastbound internal lanes may share the same features, but offset and travel time (defined in next section) will have different influence on them, while offset have the hysteresis on westbound internal lane just like travel time do, conversely, travel time and offset have opposite impact on the eastbound internal lane, as shown in Figure 3-8. In the Figure 3-8, (a) that show eastbound, the inflows are controlled by 14&7 and 2&4, the ring 1 in black represents the original timing plan, while offset render the inflow arrive earlier by moving those two signal groups to the left, result in red one which is the final timing plan, the travel time lead ring 1 shift to right as

shown in green which is the actual arriving timing plan used for calculation. However, in Figure 3-8 (b), both offset and travel time play a role to shift the original arriving plan to right and form the actual arriving timing plan which marked in green. So the delay of westbound and eastbound internal lane should be calculated separately.

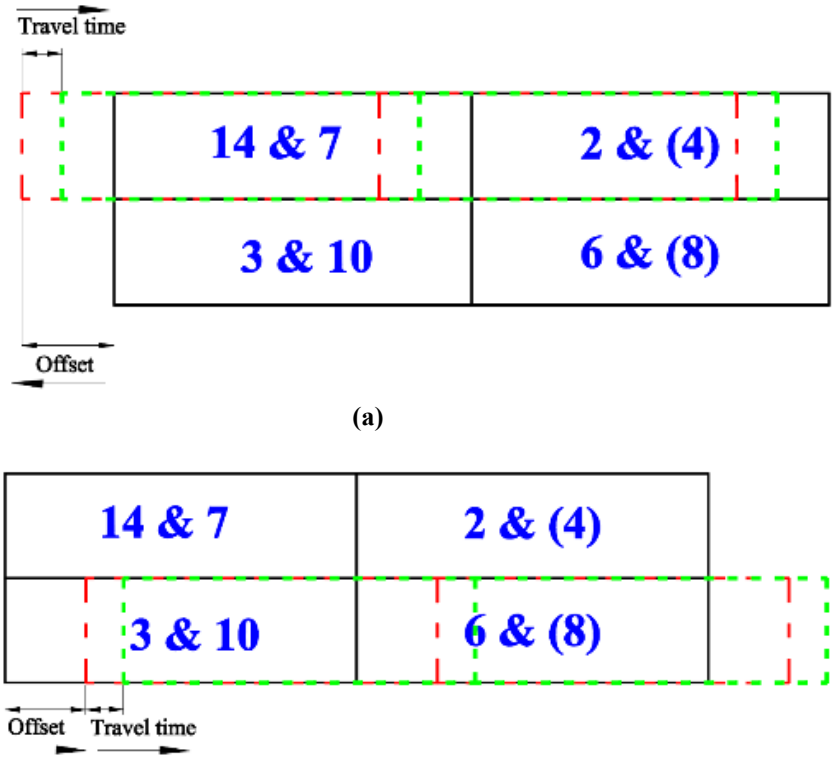

Figure 3-8 Different influence of offset and travel time on westbound and eastbound internal lane, (a) is eastbound, (b) is westbound

(1) Only undersaturated traffic are considered:

In the reality and practice, in order to avoid oversaturated delay, the timing plans are created to ensure the capacity is greater than arrival rate in each cycle, hence keep the traffic under undersaturated condition. Since the proposed delay calculation in this study

aim to help develop the optimized timing plans, only undersaturated traffic scenarios are considered.

3.4.2 Delay Calculation of Westbound Internal Lane

The first step is to set up the input parameters, length of internal lane denoted by L, desired speed on the internal lane denoted by v_L, saturated flow of each approach S_i, which controlled by signal group i, and amber and all red time r_L. Offset and Travel time on the internal lane determine which upstream traffic flow will serve as inflow to internal lane first when the light control internal lane turn red. Lag denotes the amount of time the first inflow served during the red time of internal lane. For westbound internal lane, this is controlled by phases 14&7. Offset changes the difference of start time between ring 2 and ring 1. Travel time alter the actual arrival pattern. For westbound specifically, there are two inflow controlled by signal group 3&10 and 6&8 which are off-ramp left turn and through movement of arterial respectively.

Travel time on internal lane is calculated as:

$$T = \frac{L}{v_L} \tag{1}$$

L is the length of the internal lane, v_L is the desired travel speed on the internal lane, and T is travel time on the internal lane.

Effective green time G, and effective red time R for westbound internal lane

$$R = G_{2\&4} + 2r_L, G = G_{7\&14} \tag{2}$$

Lag is the amount of time the first inflow served during the red time of internal lane,G_i is the effective green time of approach controlled by signal group i, the first served

inflow change with the offset, travel time and effective green time, and red time, which are shown below.

Inflow from ramp that controlled by 3&10 will serve first when

$$\text{Lag} = \left\{ \begin{array}{c} \mathrm{O} + \mathrm{T} + G_{3\&10} + \mathrm{r}_L - G_{14\&7} - C \\ (G_{14\&7} - G_{3\&10} - \mathrm{r}_L + \mathrm{C} \le \mathrm{O} + \mathrm{T} \le G_{14\&7} + C) \\ \mathrm{O} + \mathrm{T} + G_{3\&10} + \mathrm{r}_L - G_{14\&7} \\ (G_{14\&7} - G_{3\&10} - \mathrm{r}_L \le \mathrm{O} + \mathrm{T} \le G_{14\&7}) \end{array} \right\} \quad (3)$$

$$g_1 = G_{3\&10}, g_2 = G_{6\&8}\,, s_1 = s_{3\&10}, s_2 = s_{6\&8}, q_1 = q_{3\&10,}\, q_2 = q_{6\&8} \quad (4)$$

Inflow from arterial that controlled by 6&8 will serve first when

$$\text{Lag} = \left\{ \begin{array}{c} \mathrm{O} + \mathrm{T} + G_{2\&4} + 2\mathrm{r}_L \\ (O + T < G_{14\&7} - G_{3\&10} - \mathrm{r}_L) \\ \mathrm{O} + \mathrm{T} - G_{14\&7} \\ (G_{14\&7} < O + T < G_{14\&7} - G_{3\&10} - \mathrm{r}_L + C) \\ \mathrm{O} + \mathrm{T} - G_{14\&7} - C \\ (O + T > G_{14\&7} + C) \end{array} \right\} \quad (5)$$

$$g_1 = G_{6\&8}, g_2 = G_{3\&10}\,, s_1 = s_{6\&8}, s_2 = s_{3\&10}, q_1 = q_{6\&8,}\, q_2 = q_{3\&10} \quad (6)$$

O is the offset, which is defined as the difference between the start time of signal group 3&10 and 14&7. g_1 is the effective green time of upstream signal that control the first served inflow. g_2 is the effective green time of upstream signal that control the second served inflow. C is cycle length. s_1 is the saturated flow of the upstream flow serve first. s_2 is the saturated flow of the upstream flow serve next. q_1 is arrive rate of upstream flow serve first. q_2 is arrive rate of upstream flow serve next.

The total delay area is divided into 9 parts, but they will not exist simultaneously. The value of each part depends on the Lag and traffic from upstream:

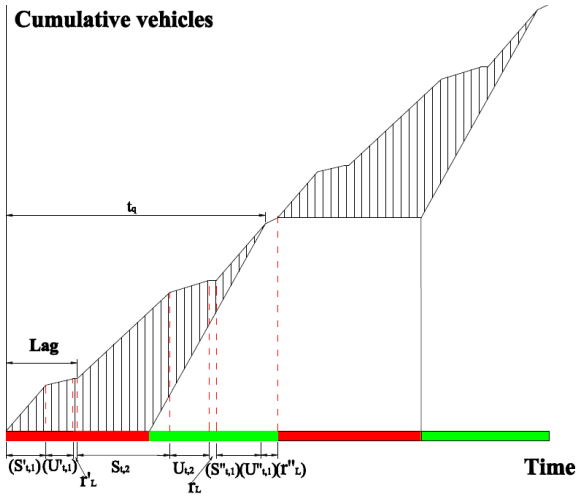

Figure 3-9 Delay calculation diagram

Under undersaturated flow, $S_{t,1} < g_1,\ S_{t,2} < g_2$

$$S_{t,1} = \frac{(C-g_1)q_1}{s_1-q_1}, \text{ s.t: } S_{t,1} < g_1 \tag{7}$$

$$r'_L = \min(Lag, r_L),\ r''_L = r_L - r'_L \tag{8}$$

$$U_{t,1} = g_1 - S_{t,1} \tag{9}$$

$$S_{t,2} = \frac{(C-g_2)q_2}{s_2-q_2}, \text{ s.t: } S_{t,2} < g_2 \tag{10}$$

$$U_{t,2} = g_2 - S_{t,2} \tag{11}$$

$$U'_{t,1} = \max[\min(U_{t,1}, \text{Lag} - r_L), 0],\ U''_{t,1} = U_{t,1} - U'_{t,1} \tag{12}$$

$$S'_{t,1} = \max(Lag - U'_{t,1} - r_L, 0),\ S''_{t,1} = S_{t,1} - S'_{t,1} \tag{13}$$

$S_{t,1}$ is the time period of the saturated flow of the first served upstream movement, $S'_{t,1}$ is the first period of $S_{t,1}$ that included in Lag and appear on the left the diagram, $S''_{t,1}$ is the second period of $S_{t,1}$ out of Lag and appear on the right of diagram, $U_{t,1}$ is the time period of the unsaturated flow of the first served upstream movement, $U'_{t,1}$ is the first period of $U_{t,1}$ that is included in Lag and appear on the left the diagram, $U''_{t,1}$ is the second period of $U_{t,1}$ out of Lag and appear on the right of diagram, $U_{t,2}$is the time period of the

unsaturated flow of the second served upstream movement, $S_{t,2}$is the time period of the saturated flow of the second served upstream movement.

In order to consider all scenarios into a uniform calculation, and for the convenience to program, the intermediate variable are calculated and used

$$f_1 = S'_{t,1}, f_2 = U'_{t,1}, f_3 = r'_L, f_4 = S_{t,2}, f_5 = U_{t,2}, f_6 = r_L, f_7 = S''_{t,1}, f_8 = U''_{t,1}\ f_9 = r''_L \quad (14)$$

$$v_1 = s_1, v_2 = q_1, v_3 = 0, v_4 = s_2, v_5 = q_2, v_6 = 0, v_7 = s_1,\ v_8 = q_1, v_9 = 0 \quad (15)$$

$$p_n = \sum_{j=1}^{n} f_j \qquad n = 1,2,3,4,5,6,7,8,9 \quad (16)$$

$$V_n = \sum_{j=1}^{n} f_j\, v_j \quad n = 1,2,3,4,5,6,7,8,9 \quad (17)$$

f_i is the time duration flow i served, p_i is the cumulative time when flow i end, v_i is the flow rate of flow i, V_i is the accumulative arrival at the end of flow i served, timing start when signal that control internal turn red.

t_q is the time that queue served, which is calculated

$$i = \min(n), \text{enable } (p_n - R)s > V_n, n = 1,2,3,4,5,6,7,8,9 \quad (18)$$

$$t_q = \begin{cases} \frac{V_{i-1} - (p_{i-1} - R)s}{s - v_i} + p_{i-1} & p_{i-1} > R \\ \frac{V_{i-1} + (R - p_{i-1})v_i}{s - v_i} + R & p_{i-1} < R \end{cases} \quad (19)$$

As the cumulative arrival curve and cumulative departure curve shown in Figure 3-9, the delay can be calculated as the area between those two curves, which are marked as shadow in the figure.

$$d_n = \frac{[(V_{n-1} + V_n)f_n]}{2}, n = 1,2,3,4,5,6,7,8,9 \quad (20)$$

$$D = \left[\sum_{j=1}^{i-1} d_j - \frac{(t_q - R)^2 S}{2} + \frac{[(t_q - p_{i-1})v_i + 2V_{i-1}](t_q - p_{i-1})}{2}\right] / V_8 \quad (21)$$

3.4.3 **Delay Calculation of Eastbound Internal Lane**

The delay calculation of eastbound internal lane differs from westbound on the determination of first served inflow and Lag period, result from the opposite influence of travel time and offset, and different controlling signal groups, since travel time lead inflow arrive later while offset make them earlier for eastbound internal lane.

$$\mathrm{R} = G_{6\&8} + 2r_L, \mathrm{G} = G_{3\&10} \tag{22}$$

$$Lag = \left\{ \begin{array}{c} G_{6\&8} - (\mathrm{O} - \mathrm{T}) + 2r_L \\ (G_{14\&7} - \mathrm{G}_{3\&10} + r_L \ \leq \mathrm{O} - \mathrm{T} \leq G_{6\&8} + 2r_L) \\ G_{6\&8} - (\mathrm{O} - \mathrm{T}) + 2r_L - C \\ (G_{14\&7} - \mathrm{G}_{3\&10} + r_L - \mathrm{C} \leq \mathrm{O} - \mathrm{T} \leq G_{6\&8} + 2r_L - C) \end{array} \right\} \tag{23}$$

$$g_1 = G_{2\&4}, g_2 = G_{14\&7,} s_1 = s_{2\&4}, s_2 = s_{14\&7}, q_1 = q_{2\&4,}\ q_2 = q_{14\&7} \tag{24}$$

$$\mathrm{Lag} = \left\{ \begin{array}{c} G_{14\&7} \ - (O - T) - G_{3\&10} + r_L \\ (G_{6\&8} + 2r_L - C < \mathrm{O} - \mathrm{T} < G_{14\&7} - G_{3\&10} + r_L) \\ G_{14\&7} \ - (O - T) - G_{3\&10} + r_L - C \\ (\mathrm{O} - \mathrm{T} < G_{14\&7} - G_{3\&10} + r_L - C) \\ G_{14\&7} \ + G_{6\&8} - (O - T) + 3r_L \\ (\mathrm{O} - \mathrm{T} > G_{6\&8} + 2r_L) \end{array} \right\} \tag{25}$$

$$g_1 = G_{14\&7,}\ g_2 = G_{2\&4}, s_1 = s_{14\&7}, s_2 = s_{2\&4}, q_1 = q_{14\&7,}\ q_2 \ = q_{2\&4} \tag{26}$$

Then with (7) to (21), the average delay of is calculated.

The basic logic of delay calculation on internal lane are shown in Figure 3-10.

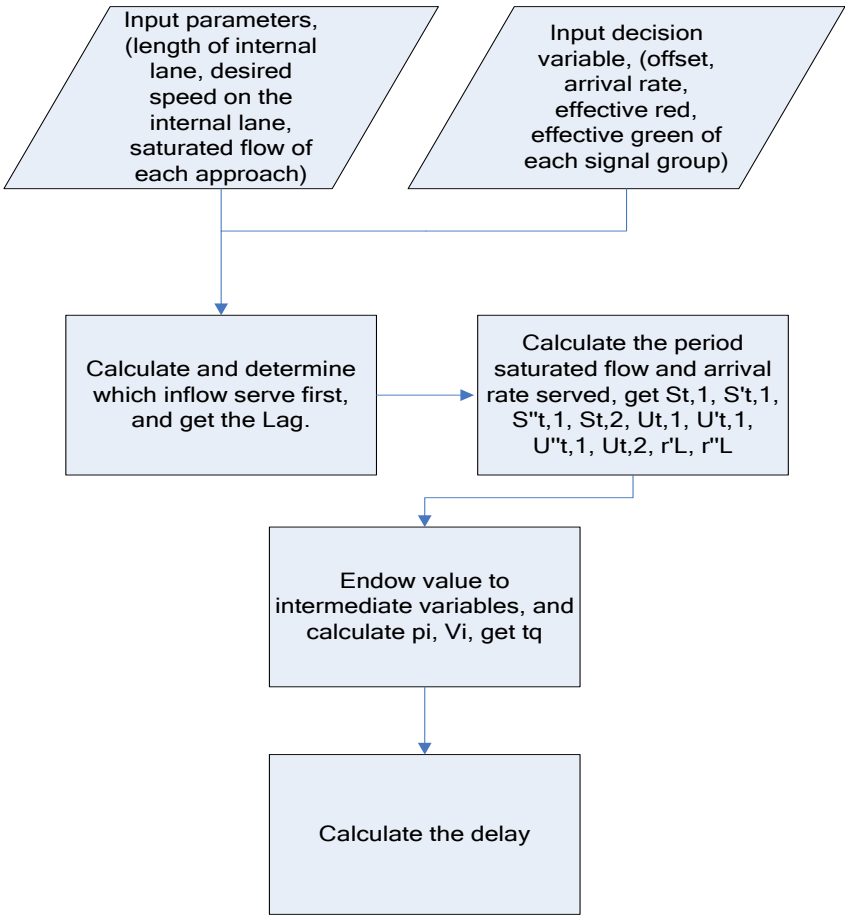

Figure 3-10 Flow Chart of Calculation Logic

3.5 SIMULATION AND VERIFICATION

VISSIM 7.0 was used to verify the calculations, since it is capable of creating all kind of configuration of the network and can provide options to change basic setting such as the speed distribution. In the calculation, the length of internal lane is set to be 178m, desired speed is 11.11m/s, $s_{2\&4} = s_{6\&8} = 6000$veh/h,$s_{3\&10} = s_{14\&7} = 4000$veh/h, since DDI present different configuration from traditional intersection, in which the conflict area is comparative smaller than normal intersection, amber and all-red time are set to be 2s.

JMP design of experiment module was used to create traffic patterns with variables that can adequately represent the full response surface for a robust experimental analysis. 8 variables were chosen as input:C,$G_{14\&7}$,$G_{3\&10}$,$q_{3\&10}$,$q_{6\&8}$, $q_{2\&4}$,$q_{14\&7}$, and offset. Since $G_{2\&4,}$ $G_{6\&8}$ can be calculated from are C, $G_{14\&7}$ and $G_{3\&10}$, 10 variables were put into each pattern. The input to JMP is shown in Table 3-3. In which d_i are the origin input into JMP, d'_i are the final input to calculation and simulation by altering d_i.

Table 3-3 Input Variable for JMP

Parameters / Value	**C**	**$G_{14\&7}$**	**$G_{3\&10}$**	**$q_{3\&10}$**
d_i	30-120 Step 10	0.3-0.7 Step 0.05	0.3-0.7 Step 0.05	0.1-0.3 Step 0.05
d'_i	$d_1 + 2r_L$	$C \cdot d_2$	$C \cdot d_3$	$S_{3\&10} \cdot d_4$
Parameters / Value	$q_{6\&8}$	$q_{2\&4}$	$q_{14\&7}$	offset
d_i	0.1-0.3 Step 0.05	0.1-0.3 Step 0.05	0.1-0.3 Step 0.05	0-0.9 Step 0.1
d'_i	$S_{6\&8} \cdot d_5$	$S_{2\&4} \cdot d_6$	$S_{14\&7} \cdot d_7$	$d_1 \cdot d_8$
Parameters / Value	$G_{2\&4}$	$G_{6\&8}$		
d_i	-	-		
d'_i	$d_1 - d'_2$	$d_1 - d'_3$		

JMP produced a total of 39 different patterns. By inputting those patterns into VISSIM and the spreadsheet that contains the proposed equations respectively, comparisons were made for delay calculation of westbound internal lane, eastbound internal lane and total delay of those two directions with simulation, which are shown in Figure. 3-11, Figure 3-12 and Figure 3-13.

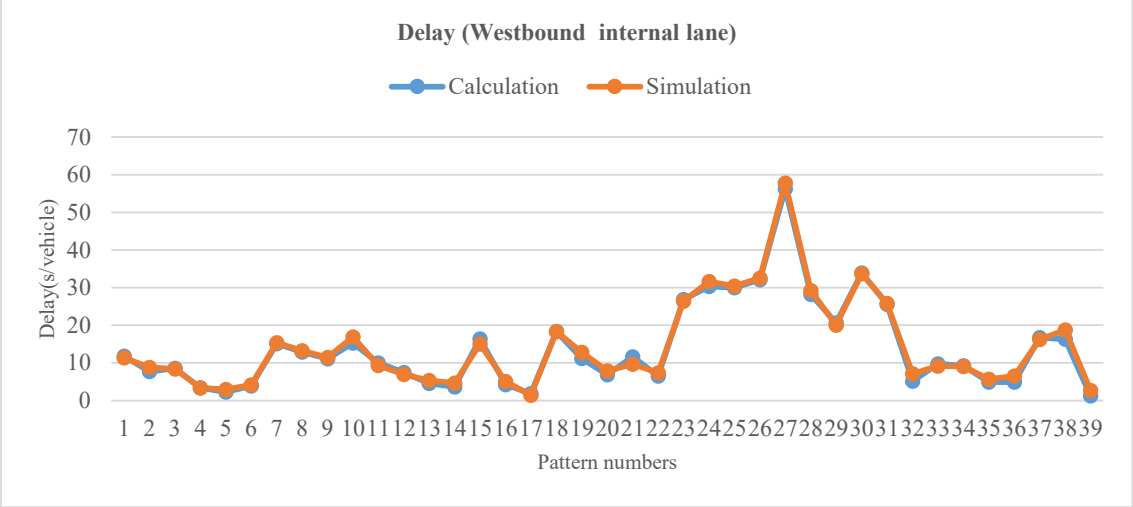

Figure 3-11 Comparison for Westbound Internal Lane

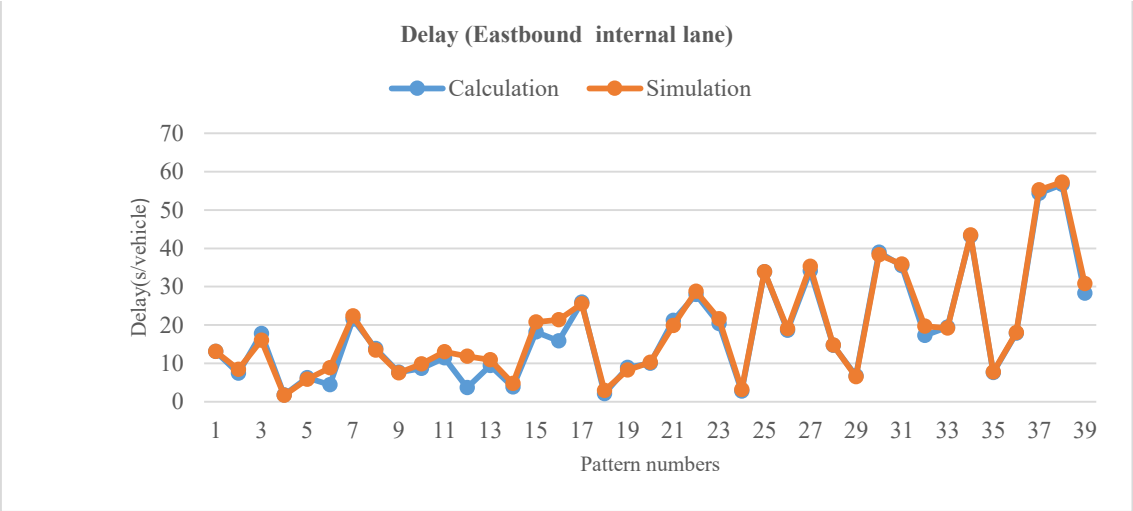

Figure 3-12 Comparison for Eastbound Internal Lane

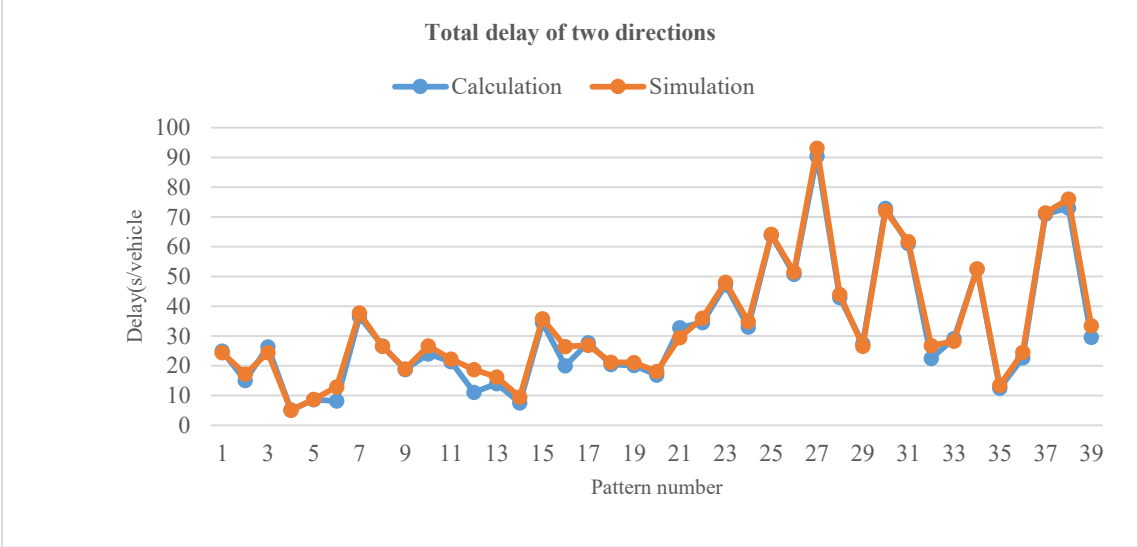

Figure 3-13 Comparison of total delay of those two directions

The R-Square are shown in Table 3-4.

Table 3-4 . R-Square of Results

Direction / Value	Westbound	Eastbound	Total
R-Square	0.996764	0.991385	0.99493

CHAPTER 4 SAFETY ASSESSMENT OF ECODRIVING VEHICLES ON FOLLOWING TRAFFIC

Xi Duan
Charles Via Department of Civil and Environmental Engineering
301-D, Patton Hall
Virginia Polytechnic Institute and State University
Blacksburg, VA, 24061
E-mail: xiduan@vt.edu

Montasir M. Abbas, Ph.D., P.E. (Corresponding Author)
Associate Professor
Charles Via Department of Civil and Environmental Engineering
301-A, Patton Hall
Virginia Polytechnic Institute and State University
Blacksburg, VA, 24061
Phone: (540) 231-9002
E-mail: abbas@vt.edu

4.1 ABSTRACT

Ecodriving aims to achieve the best fuel efficiency by guiding vehicles travel at planned and optimized speed trajectory, mainly achieved by taking better use of topography and signal phasing and timing (SPaT) information. Previous work mainly put emphasis on the development of ecodriving algorithm or on the assessment of its efficiency. However, few research efforts has been done in respect of safety of ecodriving. In this paper, instead of trying to increase the ecodriving safety by incorporating constraints into ecodriving algorithm, it opens the door for safety concerns for following normal driving vehicles (FNVs) when following ecodriving vehicles (EVs). To examine the safety issues under different circumstance. Three road elements: initial signal status, ambient vehicles and speed limit along with three EV elements: SpeedTolimit, DistanceToStoplight and acceleration were chosen as potential influential elements, and time to collision (TTC) was selected as the dependent variable. Therefore, six testing scenarios and six baseline were designed and implemented using a drive safety DNS-250 simulator. 29 drivers participated in the driving simulator study. The results show the aforementioned road elements and EV elements have significant influence on TTC of FNV in different testing parts. Therefore, these finding can be used as guidance for future ecodriving algorithm design and implementation.

Keywords—ecodriving, initial signal part, safety, TTC

4.2 INTRODUCTION

In sum, the aforementioned research focused either on the ecodriving algorithm development itself, or on the assessment of ecodriving efficiency. Nevertheless, safety issues aroused by implementation of ecodriving are not of concern. Although some studies involved safety indicator such as TTC into their ecodriving algorithm as a constraint [14, 16, 17], which prevents the EVs and other NVs (normal-driving vehicles) from reaching certain dangerous circumstance when following another vehicle. However, in their models, constrained TTC was assumed to be same as usual (traffic without EV) or a constant which may result in inconformity with reality. Besides, all those studies only considered the safety issues from EVs' perspective, few research efforts has been put on the safety assessment of following normal-driving vehicles (FNVs) when following an EV, which present abnormal driving behaviors from FNVs perspective. For instance, the EVs will start decelerating further away from intersections even when the signal is still on green as knowing it cannot pass the intersection within the current green phase; it may also decelerate and accelerate smoother than usual to avoid hitting the red light when arrives at the stoplight. These unusual driving behaviors might result in potential risks for FNVs that without the knowledge of that the leading vehicle is an EV. For example, FNVs are likely to follow the EVs closer than usual or do not even response in time when the EV ahead start decelerating as they are not anticipating the preceding EV will start decelerating when the signal ahead is still on green. Those critical car-following circumstance could be reflected with the TTC value of FNVs when following an EV.

This research opens the door for safety concerns of FNV that are following EV. In this paper, the power- based longitudinal ecodriving algorithm was formulated first in the

section II with the objective to minimize the fuel consumption without compromising the travel time. In the section III, the design and implementation of experiments are introduced. 12 scenarios were developed with the purpose to examine the influence of elements such as initial signal status, speed limit and ambient vehicles on the car-following behavior of drivers following EV. During the test, 29 volunteers attended the simulator driving test. The second-by-second data are collected by Drive-Safety DS-250 with specified code and the data analysis was done by SPSS. Analysis are done in section IV, analysis of variance, regression, numerical and graphical comparisons are conducted to examine the influence of road elements and EV elements on TTC. The conclusions are reached in section V and suggestion for future research are put forward in section VI.

4.3 ECODRIVING ALGORITHM

The ecodriving algorithm used in this research is a power-based longitudinal control algorithm, which aims to minimize the fuel-consumption without increasing the travel time. The whole optimization is composed of 2 horizons (Figure 4-1): the upstream horizon and downstream horizon. The upstream horizon (deceleration part) is where the EVs entered at an initial speed and then decelerate to travel for a certain distance to pass through the first intersection at specified time. Another horizon is downstream horizon (acceleration part), in which EVs are supposed to accelerate to travel a certain distance in a certain time period in order to exit the second intersection at the desired speed.

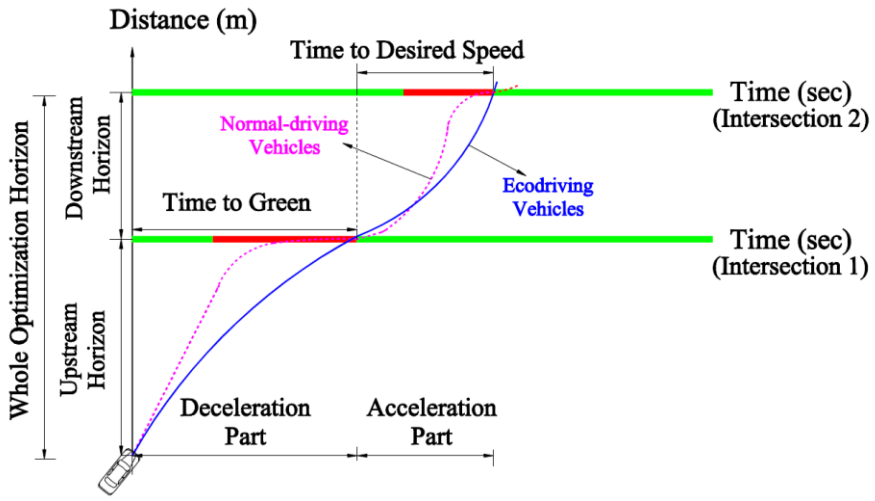

Figure 4-1 Optimization Horizon Layout

The ecodriving algorithm used in this paper has four assumptions.

1. The high fuel efficiency is achieved without compromising the travel time, which means the EV will always take the first window of green phase to pass intersections if possible.

2. The influence of downstream vehicles on the EV are not considered in this model, as the purpose of this research is to examine the following behavior of the FNV following the EV. Therefore, it is assumed no vehicle will be traveling ahead of EV. Variation caused by downstream vehicles hence will be controlled with this constraint.

3. The speed trajectory is developed second-by-second, and acceleration and deceleration are constant during each time interval.

4. The ecodriving control algorithm will only be implemented when the EV are predicted to hit the red light if they maintain the current speed.

The Objective function of this ecodriving algorithm is to minimize fuel consumption.

$$Min \sum_{i=1}^{T} F(i) \quad (27)$$

$F(i)$ (l/s) is the fuel consumption for each time step.

Acceleration $A(i)$ is calculated by the difference in speed for 2 consecutive seconds.

$$A(i) = \frac{V(i)-V(i-1)}{3.6} \tag{28}$$

$V(i)$ (km/h) is the speed for each time step. $V(0)$ (km/h) is the initial speed.

The EV must travel the length of the upstream horizon at a certain time (time to green).

$$\sum_{i=1}^{T_G} \mathrm{V}_i/3.6 = \mathrm{L}_U \tag{29}$$

$\mathrm{L_U}$ (m) is the distance of the upstream horizon. $\mathrm{T_G}$ (s) is the time to green, which starts when the EV enter the optimization horizon (Fig.1) then ends with the next green phase.

The EV must travel the distance of downstream horizon at a certain time (time to desired speed).

$$T = T_G + T_D \tag{30}$$

$$\sum_{i=T_G}^{T} \mathrm{V}_i/3.6 = \mathrm{L}_D \tag{31}$$

T (s) is the total time of the whole ecodriving optimization horizon. T_D (s) is the time to desired speed, within which EV should accelerate to desired speed (Figure 4-1). It starts when EV enter the downstream horizon and ends when EV exit it. $\mathrm{L_D}$ (m) is the length of downstream horizon.

EV must reach the desired speed when they exit the downstream horizon.

$$\mathrm{V}_T \geq V_d \tag{32}$$

V_T (km/h) is the velocity of EV when exiting the optimization horizon. V_d (km/h) is the desired speed of EV which is usually set to be speed limit.

The power-based longitudinal ecodriving algorithm was chosen in this research because of its ability algorithm is able to take the vehicle dynamics, road grade, and other road parameters into consideration. The instant required power of EV is calculated as:

$$P(i) = \frac{R(i)+1.04m\times A_i}{3{,}600\eta_d} V_i, \ \forall \mathrm{i} \in \mathrm{T} \tag{33}$$

$P(i)$ (Horsepower) is the instant power of EV, η_d is the driveline efficiency. The output power for each instant is constrained by the maximal power of vehicles.

$$p(i) \leq p_M, \ \forall \mathrm{i} \in \mathrm{T} \tag{34}$$

p_M (Horsepower) is the maximal output power of EV.

The resistance of the EV when traveling on the road is composed of aerodynamic, rolling, and grade resistance forces and is calculated as"

$$R(i) = \frac{p}{25.92} C_D \ C_h A_f {V_i}^2 + 9.8066m\frac{c_1}{1000}(c_2 V_i + c_3) + 9.8066mG(i), \quad \forall i \in T \tag{35}$$

$R(i)$ (N) is the resistance force, p is density of air at sea level at a temperature of $15^{\mathrm{o}}\mathrm{C}$, C_D is vehicle drag coefficient, typically 0.30; C_h is correction factor for altitude H (km), which is computed as $1 - 0.085H$; A_f (m^2) is vehicle frontal area; c_1, c_2, c_3 are rolling resistance parameters, $G(i)$ is roadway grade at instant i. m (kg) is the mass of EV.

The velocity of EV for each instant must conform to the speed limit; the acceleration of EV for each instant must be lower than the desired deceleration rate.

$$\mathrm{V(i)} < \mathrm{V}_L \ , \ \ \forall \mathrm{i} \in \mathrm{T} \tag{36}$$

$$\mathrm{A(i)} < \mathrm{A}_{LA}, \ \forall \mathrm{i} \in \mathrm{T} \tag{37}$$

$$A(i) > A_{LD}, \ \forall i \in T \tag{38}$$

V_L (km/h) is the speed limit, A_{LA} (m/s^2) is the desired acceleration level and A_{LD} (m/s^2) is the desired deceleration level. According to the Traffic Engineering Handbook, the average deceleration and acceleration values at an intersection stoplight are -3 m/s^2 and 1.1 m/s^2, respectively.

The power based fuel consumption at a given time step *t* is then calculated as:

$$F(i) = \begin{cases} \alpha_0 + \alpha_1 p(i) + \alpha_2 p(i)^2 & \forall p(i) \geq 0 \\ \alpha_0 & \forall p(i) \leq 0 \end{cases} \tag{39}$$

α_0, α_1, α_2 are coefficients that were obtained using VT-CPFM software [21].

This power-based ecodriving algorithm could be extended by making the initial speed to be the same as desired speed exited from the last optimization horizon.

4.4 EXPERIMENTAL DESIGN

4.4.1 Purpose of the Experiments

The experimental design should be comprehensive and be able take varied travel status of EVs into consideration in order to identify critical circumstance. The parameters setting should be typical to conform to reality, at the same time, be extreme among the typical range to assure enough data collection.

Generally, EV will accelerate and decelerate smoother than NV. In this sense, following an EV is even safer than following a NV. However, in order to make better use of the SPaT information, EV will decelerate further away from the intersection even when signal is still on green. Besides, EV will accelerate slower than usual to pass through another intersection without hitting the red light. However, these behaviors are unanticipated by

following drivers without the knowledge that leading vehicles are EV, which will result in critical car-following circumstance.

In order to quantify the danger degree, time to collision (TTC) is chosen as it is the most well-known time-based safety indicator. TTC refers to the time remaining before the rear-end accident if both the course and speed of preceding and following vehicles are maintained. Previous research concluded that the TTC is an effective measure for discriminating critical from normal behaviors in car-following situations [22]. TTC value at an instant *i* is defined as the remaining time for two vehicles to collide if both of they continue at their current speed and on the same path. Therefore, the higher a TTC value, the safer a situation.

The experiments are designed with the purpose of identifying the influence of predefined road elements on the TTC of FNV when following an EV, and comparing them to the situations when following a NV. In these experiments, the leading EV and NV are designed to complete both deceleration and acceleration behaviors to fully achieve the experimental purpose.

4.4.2 Road and EV Elements Considered

In this study, only the car-following behavior will be examined while lane-change behavior is out of range. Therefore, three road elements along with three EV elements were considered that could have potential influence on TTC of FNV when following EV (Table 4-1).

Table 4-1 Road Elements Types and Levels

Classification	Types	Elements	Levels
Road Elements	Categorical	Ambient Vehicles	1. Ecodriving vehicle

			2. Normal driving vehicle 3. No vehicle
		Speed Limit	1. 35 MPH 2. 40 MPH 3. 45 MPH
		Initial Signal Status	1. Green 2. Red
EV Elements	Numerical	DistanceTo Stoplight	Continous
		SpeedToSpeed Limit	Continous
		Acceleration	Continous

Ambient vehicle is the vehicle lateral to the EV, which is followed by FNV (subject). The ambient vehicle can be either an EV, NV or no car (Figure 4-2). This element is set to examine if the different ambient vehicles will impact the following behaviors of FNVs. Three speed limit level which vary from 35 MPH to 45 MPH are considered. These are the typical speed limit setting of signalized urban area. The initial Signal status is the signal status ahead when EV enter the optimization horizon (upstream horizon or downstream horizon), which is shown in Figure 4-1. Because ecodriving control will only be implemented when EVs are predicted to hit the red light if maintain at current speed. Thus, the length of initial green time should have two considerations. First, the initial green time should be set as long as possible to enable enough data collection in initial signal part. Secondly, the initial green time should not that long within which the EVs can pass through the intersection. DistanceToStoplight is the instant distance between the EV and the stop line of the preceding intersection. SpeedToLimit is the difference between EV's instant speed and the speed limit of the current road. Acceleration is the EV's instant acceleration.

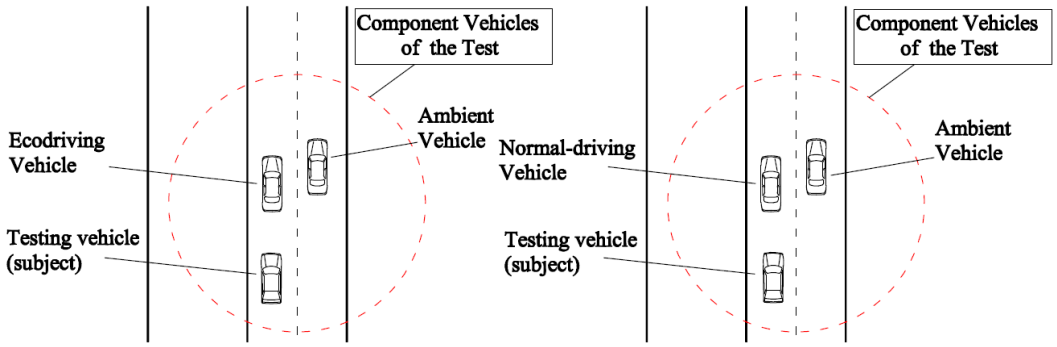

Figure 4-2 Components Vehicles

4.4.3 Implementation

(1) Scenarios Design

The first three elements shown in Table 4-1 are road elements, each of their levels should be incorporated in the experimental designs. Nevertheless, the three other EV elements can be extracted from any scenario without specification in experimental designs. Therefore, the EV elements are out of concern in the designing horizon. Three levels of ambient vehicles, three levels of speed limit and two levels of initial signal status are involved into experimental designs. JMP is used for this purpose and six scenarios are generated, which are shown in Table 4-2. Besides, the six baseline scenarios are developed by replacing the EVs with NVs. (Figure 4-2).

Table 4-2 Scenarios Design

Scenarios Designs			
Scenarios	Speed Limit	Initial Signal	Ambient Vehicle
1	45 MPH	Red	No car
2	40 MPH	Red	Normal
3	40 MPH	Green	Eco
4	35 MPH	Red	Eco

5	45 MPH	Green	Normal
6	35 MPH	Green	No car

(2) Parameters Setting

In respect of signal design for the experiments, it is composed of four parts: the initial signal time of signal 1, remaining red time of signal 1, initial signal time of signal 2 and remaining red time of signal 2 (Figure 4-3). The initial green time should be as long as possible for enough data collection while being shorter enough to make sure the EV cannot cross the intersection at the speed limit. Thus it can be calculated as:

$$\mathrm{G}_i = D_e/V_L - 1 \tag{40}$$

G_i (s) is the initial green time of each horizon for scenarios whose initial signal are set to be green. D_e(m) is the length of each horizon. Thus, in scenario 3, 5 and 6 whose initial signal status are green, the green times are set to be14s and 8s for the initial signal part 1 and initial signal 2 respectively. The length of time to green of signal 1 is set to render EV decelerate to pass the stop line of intersection 1, while time to desired speed of signal 2 makes EV then accelerate to pass through intersection 2. The signals' phasing and timing is designed for testing purpose hence only the signal time of the preceding signal before EV pass through intersection that could have influence on subjects are specified (Figure 4-3). The total duration of each scenario is 59 seconds. The first 39-second is deceleration part (upstream horizon), where EVs will decelerate to pass through the first intersection since entered the optimization horizon. The followed 20-second is acceleration part (downstream horizon) where vehicles will accelerate to desired speed to pass through the second intersection from the first intersection.

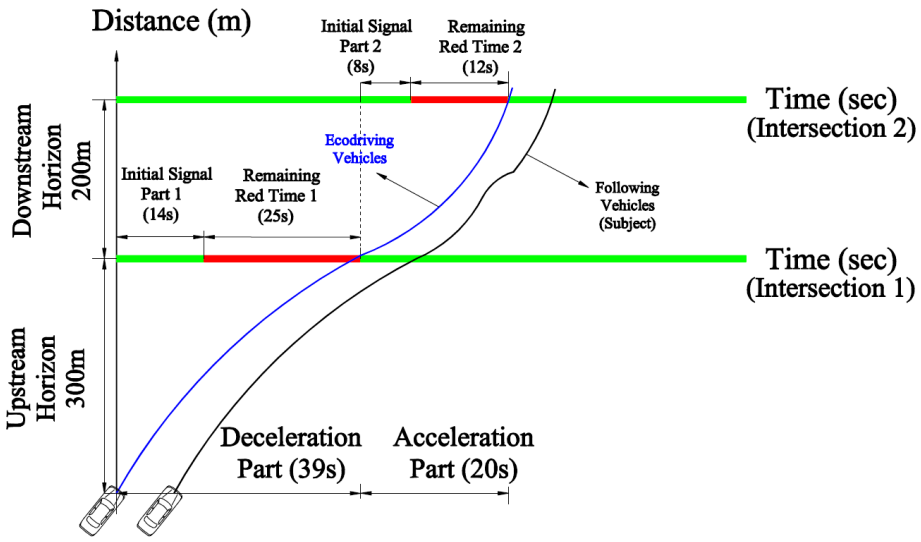

Figure 4-3 Parameters Setting

The whole optimization horizon is set to be 500 meters, which is comprised of 200-meter upstream horizon and 300-meter downstream horizon. Those lengths are designed according to the visibility of each stoplight with mast arm and the designing purposes of each horizon. In this research, a Camry 2011 model was chosen; whose specification was put into VT-CPFM software to get the calibrated parameters α_0, α_1, α_2, which are 5.9296×10^{-4}, 3.4649×10^{-5} and 1.0×10^{-6} respectively. The optimized ecodriving speed trajectories were solved by Lingo16.0 with equation (1) to (13). For scenarios with different speed limit, the input parameters such as initial speed, desired speed and speed limit were changed accordingly. Thus, three different speed trajectories of EVs were developed for scenarios with different speed limit and the speed trajectories of NVs were obtained from simulator. These speed trajectories are shown in Figure 4-4.

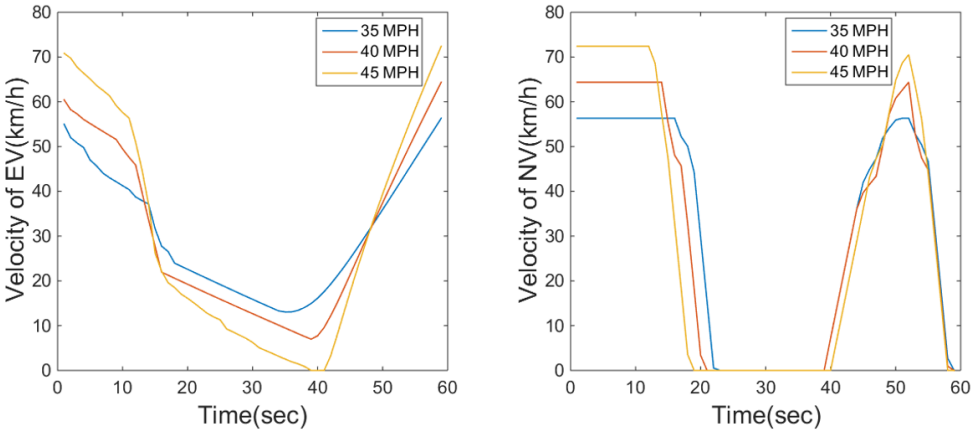

(a) **(b)**

Figure 4-4 Speed Trajectories (a) is ecodriving (b) is normal-driving

(3) Simulator driving and data collection

Drive-Safety DS-250 is used for the purpose of simulation, during which drivers sit in a partial cab based on a Ford Focus sedan and are immersed in an authentic automotive environment with simulated driving scenarios and ambient traffic (Figure 4-5)

Figure 4-5 Drive-Safety DS-250

The second-by-second speed trajectories that were solved by Lingo16.0 are further calculated for every 0.1 second assuming a constant acceleration rate during each time interval. These speed setting were then input into simulator which make the EV travel

smoothly and follow the speed trajectories accurately.

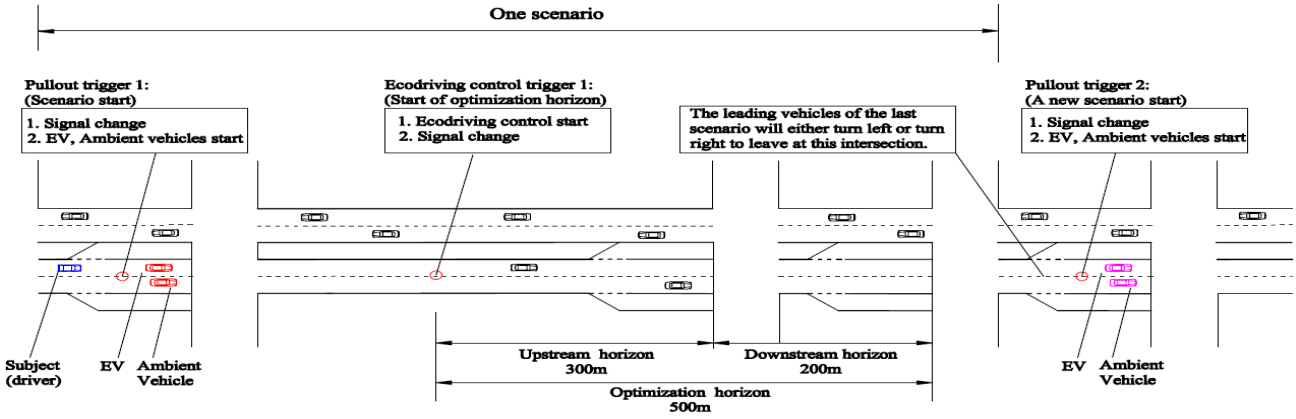

Figure 4-6 Layout of Simulation Network

For the programming process, the Triggers were used to activate signal changes and speed control for EV. The six testing scenarios and six baseline scenarios were connected to be a straight testing area and at the beginning of each scenario, the leading car stopped behind the stop line where signal is on red until subject activated the triggers and the signal turned green (Figure 4-6). This setting make sure that in every scenario, the subject will always present a car-following situation with the same start position.

29 drivers who possess valid U.S driver licenses attended the simulator driving. The second-by-second data including acceleration, speed, position of both subject (FNV) and Entity (EV), as well as some other information like TTC, system time, vehicle ahead, collision, laneindex, headway distance and headway time of subject were collected in the database.

4.5 ANALYSIS AND RESULTS

In this section, analysis of variance, regression, numerical and graphical comparisons were conducted to examine the influence of different road elements and EV elements on the TTC of FNVs following an EV as shown below.

4.5.1 Pretreatment For Time To Collision

The TTC only have value when a following vehicles travel faster than a leading vehicle when it is used under car-following circumstance. Besides, an extremely small difference in speed between a leading EV and a FNV will result in unreasonable large TTC value. However, those huge value may lead to misguide hence cannot be used directly for analysis. In other words, drivers may never realize the difference between the circumstances with such huge TTC values, since they all present the same safety level from the drivers' prospective. A previous study revealed that researchers usually consider TTC values larger than 6 sec to be safe hence were not considered in the analysis [23].Thus, 6 sec is chosen as the threshold which distinguishes safe circumstances from critical circumstances in this study. All the TTC value above 6 sec were considered as "6 or more" sec for the practicability of further analysis.

4.5.2 Examination Of Road Elements

Analysis of variance were conducted to examine the influence of road elements on TTC of FNV following an EV. After pretreated second-by-second TTC data were ready, three dependent variables were calculated: the average TTC value for each driver in the whole 59-second optimization horizon; average TTC value for each driver in the first 39-

second decelerating period (upstream horizon) and average TTC value for each driver in the followed 20-second accelerating period (downstream horizon). Then the three factors which are road elements considered in the previous scenarios design are put with every single aforementioned dependent variables in the variance analysis. All the variables have passed the homogeneity test and the F and significance value are shown in Table 4-3:

Table 4-3 Results of Variance Analysis

Dependent / Independent	Average_TTC_Overall		Average_TTC_Acceleration part		Average_TTC_Deceleration part	
	F	Sig.	F	Sig.	F	Sig.
Ambient Vehicle	1.069	.346	.093	.911	1.333	.266
Signal Status	4.685	.032	.520	.472	5.206	.024
Speed Limit	.142	.868	11.178	.000	1.066	.347

As indicated by the significance value, the initial signal status has significant impact on TTC of FNV in scope of the whole optimization horizon and the deceleration part. Moreover, the speed limit impact the TTC value significantly in the acceleration part.

Even the initial signal does not show to have significant impact on the TTC of FNV when following EV in the acceleration part, its effect could possibly be significant in the initial signal part 2, whose influence may balance by the remaining red time 2 part. Therefore, an extra regression is conducted in which the dependent variable is the averaged TTC value for each driver driving in the 8-second initial signal part 2. The significance value of initial signal status, ambient vehicles and speed limit on averaged TTC during the initial signal part 2 is 0.284, 0.171 and 0.000 respectively, the conclusions are in consistent with that of whole acceleration part.

In addition, it is necessary to know how different level of speed limit impact the TTC value as speed limit has three levels. Thus, the S.N.K. method is used for comparisons between different speed limit levels. As indicated by the results shown in Table 4-4. The averaged TTC values in the acceleration part where set speed limit at 45mph are significantly different from those when speed limit are at 35 or 45mph.

Table 4-4 Comparisons between Different Speed Limit

Speed Limit	N	Subset	
		1	2
35mph	58	5.851254	
40mph	58	5.868528	
45mph	58		5.958668
Sig.		.524	1.000

4.5.3 Check The Interaction Between Initial Signal Statuses With EV Elements.

The initial signal status is already proved to have significant influence on TTC of FNVs when following an EV in the last section. This part aims to figure out if this influence will change with EV elements, such as SpeedToLimit, DistanceToStoplight and acceleration of EV. In other words, this part seeks to check if the influence of initial signal status have interaction with those aforementioned EV elements.

Regression is used for this purpose. The dependent variables are the difference of averaged TTC for each driver in the first 14-seconds (initial signal part 1) between scenarios 1 and 5, 2 and 3, 4 and 6. Each compared group has exactly the same second-by-second SpeedToLimit, DistanceToStoplight and acceleration value of EV. The results are shown below.

Table 4-5 Coefficients of Regression

Model		Unstandardized Coefficients		Standardized Coefficients	t	Sig.
		B	Std. Error	Beta		
1	(Constant)	-.136	.033		-4.161	.000
	SpeedTolimit	.074	.009	.806	8.602	.000
a. Dependent Variable: Difference						

Table 4-6 Model Summary

Model	R	R Square	Adjusted R Square	Std. Error of the Estimate
1	.806a	.649	.640	.10846
a. Predictors: (Constant), SpeedToLimit				

As indicated by the TABLE.V, the influence of initial signal status on the TTC will change with SpeedToLimit. To be more specific, the green initial signal will cause increasing reduction on the average TTC when the speed of EV become lower compared to red initial signal.

4.5.4 Comparisons With Baseline

This part aims to quantify the influential degree of the initial signal status and speed limit on the TTC, and identify the distribution of TTC value, as they cannot be reflected by the significance value got from analysis of variance part. In addition, the TTC distributions of FNV following EV are compared to those following NV to explore how they differ from normal circumstances. Therefore, the histograms are used to describe the TTC distribution graphically for different periods: initial signal part 1, deceleration part, initial acceleration part, acceleration part and whole optimization horizon. The initial

acceleration part is defined as the first 12-second part of acceleration part when both EV and NV were accelerating during test in every scenario.

Moreover, for initial signal part 1, deceleration part and whole optimization, the histogram is draw according to different initial signal setting, while speed limit is used as the principal to divide the group in histograms for initial acceleration part and acceleration part. For the reason that the initial signal status has significant influence on initial signal part 1, deceleration part and whole optimization horizon while speed limit impact the TTC significantly in initial acceleration part and acceleration part.

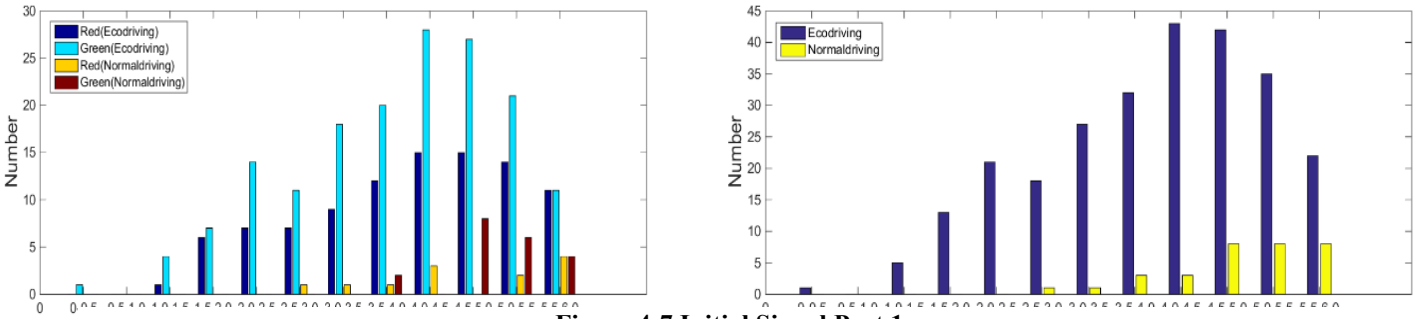

Figure 4-7 Initial Signal Part 1

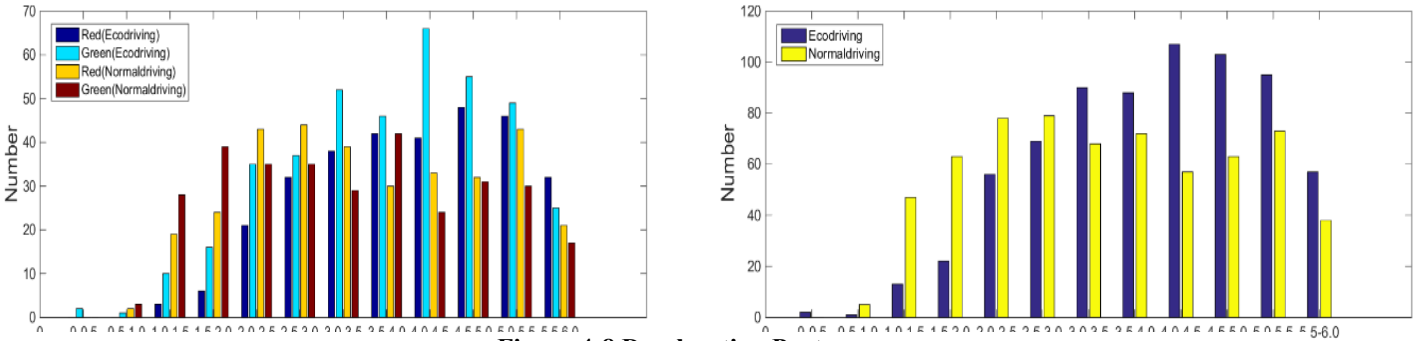

Figure 4-8 Deceleration Part

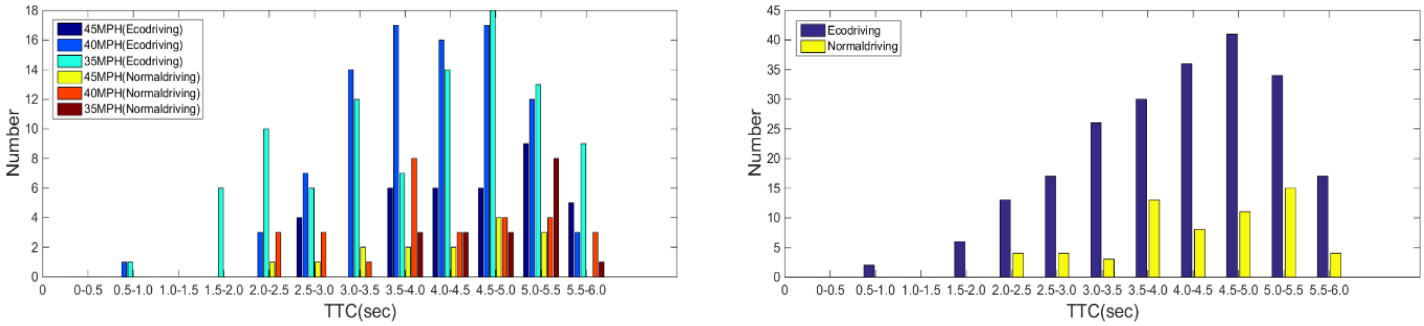

Figure 4-9 Initial Acceleration Part

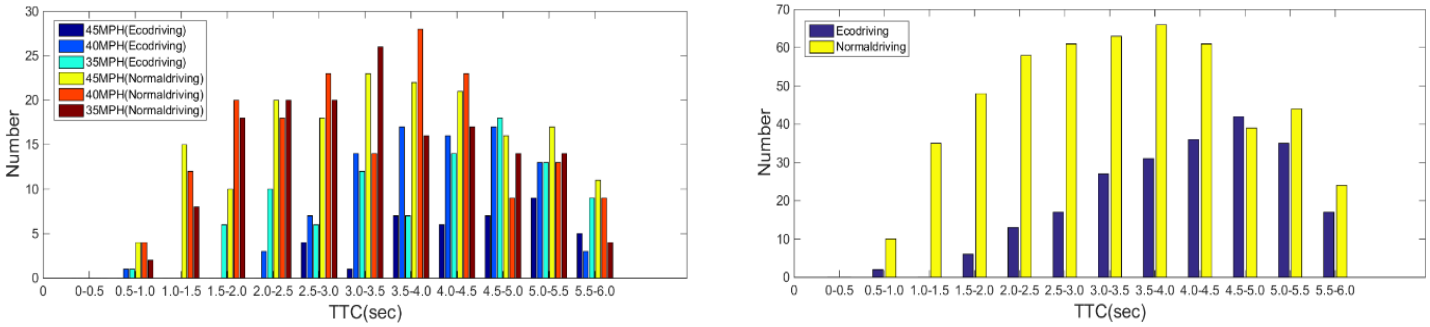

Figure 4-10 Acceleration Part

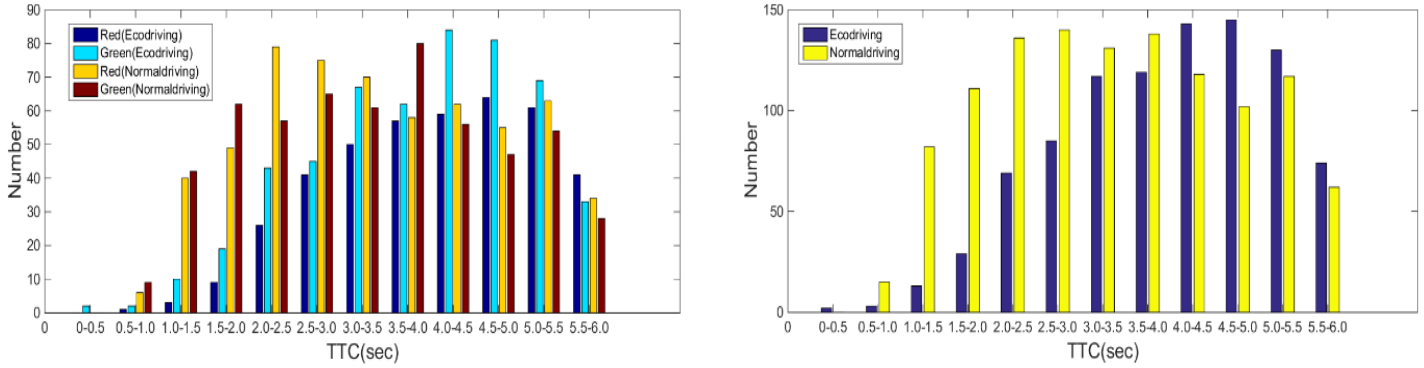

Figure 4-11 Whole Optimization Horizon

1. In the initial signal part 1, the FNV present more critical seconds (with TTC value lower than 6 sec) when following an EV than following a NV. Besides, the critical seconds are significantly more when set initial signal to be green than to be red when following an EV.

2. For the deceleration part, the impact of initial signal status on TTC of FNVs when following an EV is still significant which attribute to the remaining effects from initial signal part 1. When FNVs are following an EV compared to that following a NV, the number of seconds present larger TTC value (3.0s-6.0s) are higher. Whereas this relation is converse at lower TTC value range (0-3.0s).

3. In the initial acceleration part, the FNV that are following an EV have much more critical seconds compared to these following a NV. The number of critical seconds of FNV when following an EV are much more higher when set speed limit to be 40mph and 35mph than when the speed limit is at 45mph. Moreover, set speed limit at 35mph result in little more critical seconds than when speed limit is 40mph, especially during TTC value range of 0-2.5s.

4. In the acceleration part, following a NV is more dangerous than following an EV, as indicated by more critical seconds. When following an EV, the FNV have significantly more number of critical seconds when set speed limit at 35mph and 40 mph than when it is at 45 mph. Lower speed limit tend to result in more critical seconds.

5. For the whole optimization horizon, the influence of initial signal status on TTC of FNV when following an EV is still significant, as indicated by the more critical seconds when initial signal is green. Compared to following a NV, FNV present less number of

seconds when TTC value are at lower value range (0s-4s) while higher number of seconds when TTC range in higher value (4.0s-6.0s).

Table 4-7 Rate Of Critical Seconds For Parts With Different Initial Signal Status

	Initial Signal Part I		Deceleration	
	Red	Green	Red	Green
Normal	0.99%	1.64%	9.73%	9.22%
Eco	7.96%	13.30%	9.11%	11.61%
	Whole		Initial signal part 2	
	red	green	red	green
Normal	11.51%	10.93%	5.03%	2.59%
Eco	8.03%	10.07%	12.50%	15.09%

Table 4-8 Rates Of Different Ttc Value Range For Parts With Different Initial Signal Status

	Types	Initial signal part		deceleration	
		Red	green	red	green
0-3s	Normal	0.08%	0.00%	3.89%	4.13%
	Eco	1.64%	3.04%	1.80%	2.98%
3-6s	Normal	0.90%	1.64%	5.84%	5.10%
	Eco	6.32%	10.26%	7.31%	8.64%
	Types	whole		Initial signal part 2	
		red	green	red	green
0-3s	Normal	4.85%	4.58%	0.72%	0.43%
	Eco	1.54%	2.36%	2.01%	2.87%
3-6s	Normal	6.66%	6.35%	4.31%	2.16%
	Eco	6.49%	7.71%	10.49%	12.21%

Table 4-9 Rates Of Critical Seconds For Parts With Different Speed Limit

	Initial Acceleration Part			Acceleration Part		
	45mph	40mph	35mph	45mph	40mph	35mph
Eco	5.17%	12.93%	13.79%	3.36%	7.84%	8.28%
Normal	2.16%	4.17%	2.59%	15.26%	14.91%	13.71%

Table 4-10 Rates Of DIFFERENT TTC VALUE RANGE FOR PART WITH DIFFERENT SPEED LIMIT

		Initial Acceleration Part			Acceleration Part		
		45mph	40mph	35mph	45mph	40mph	35mph
0-3	Eco	0.57%	1.58%	3.30%	0.34%	0.95%	1.98%
	Normal	0.29%	0.86%	0.00%	5.78%	6.64%	5.86%
3-6	Eco	4.60%	11.35%	10.49%	3.02%	6.90%	6.29%
	Normal	1.87%	3.30%	2.59%	9.48%	8.28%	7.84%

4.5.5 Examination For EV Elements

The impact of road elements on TTC has been examined in previous section. In this part, EV element are evaluated through both regression and variance analysis. The analysis are conducted for deceleration part and acceleration part separately, as they present different tendency.

(1) Deceleration part

The three EV elements: second-by-second SpeedToLimit, Acceleration and DistanceToStoplight of EV are used as independent variables, and the dependent variables are the second-by-second averaged TTC values of the 29 drivers. Noting the reaction time of drivers is 1 sec so the $i\,th$ dependent variable are corresponding to the $i-1\,th$ independent variable in the regression. Therefore, the 1 sec to 39 sec independent variables' data and 2 sec to 40 sec dependent variable's data are input in SPSS with stepwise method of regression and the results are shown in Table 4-11:

Table 4-11 Coefficients Of Regression For Deceleration Part

Model		Unstandardized Coefficients		Standardized Coefficients	t	Sig.
		B	Std. Error	Beta		
1	(Constant)	5.977	0.02		297.033	.000
	Acceleration	0.509	0.034	0.815	15.086	.000

2	(Constant)	5.88	0.023		258.086	.000
	Acceleration	0.556	0.03	0.89	18.65	.000
	DistanceToStoplight	0.001	0	0.311	6.515	.000

Table 4-12 Model Summary

Model	R	R Square	Adjusted R Square	Std. Error of the Estimate
1	.815a	0.664	0.661	0.16307
2	.869b	0.755	0.751	0.13981

As inferred by Table 4-11, the impact of both acceleration and DistanceToStoplight are significant in deceleration part, The TTC of FNV when following an EV in the deceleration part will decrease with the increasing deceleration rate and decreasing DistanceToStoplight.

(2) Acceleration part

The regression of EV elements with TTC in acceleration part should be further separated into two part. Because when EV keep accelerating and get closer to the second intersection while the signal is still on red, the FNV will decelerate to avoid hitting the red light hence the car-following behaviors end. Therefore, only the first 12 seconds (initial acceleration part) are considered in the regression.

As indicated by the Table 4-13, the influence of all three EV elements on TTC during initial acceleration part are significant. The TTC will decrease as the decreasing acceleration rate, DistanceToStoplight and SpeedToLimit. However, the adjusted R square of this model is only 0.207, which means even those EV elements have significant impact on TTC, the relation may not be linear or there are other elements have not been considered.

Table 4-13 Coefficients Of Regression For Acceleration Part

Model	Unstandardized Coefficients		Standardized Coefficients	t	Sig.
	B	Std. Error	Beta		
(Constant)	5.344	.125		42.723	.000
Acc_45_red	.133	.064	.230	2.092	.040
Pos_45_red	.002	.000	.601	3.539	.001
Spe_45_red	.019	.008	.422	2.466	.016

We further notice that the acceleration rate of EV in initial acceleration part maintain constant rate which make it different from that in deceleration part. As we already know from the analysis of variance section, the speed limit has significant influence on TTC during acceleration part. So the variance analysis is conducted to test if the speed limit is correlated to the average acceleration rate.

Table 4-14 Averaged Acceleration

Value Label	Average Accleration (m/s^2)	N	Averaged TTC value (sec)
35mph	.59	24	5.851
40mph	.87	24	5.869
45mph	1.20	24	5.959

From the analysis of variance, the F value is 8.371 and the significance is 0.001, which validate the assumption that the speed limit has significant influence on TTC is result from the different acceleration rate when set at different speed limit.

4.6 FUTURE RESEARCH

Some interesting car-following behavior of FNV when following an EV are observed. During acceleration part, FNV follow EV closely, but when observing that signal is still on red but EV continuously accelerating toward intersection (knowing signal will

turn green shortly), the FNV will decelerate to make sure they can stop in front of stop line. Those interesting car-following behavior cannot be fully reflected by TTC. Acceleration or velocity based car-following models are more eligible to model those behaviors.

With the conculsion reached by this research, future study could be conducted to examine the safety of FNV following an EV with different SPaT and length of optimization horizon. These conclusion can be used as guideline for ecodriving implementation. Moreover, the minimal acceleration threshold should also be developed to avoid blocking the intersection and causing critical situations.

CHAPTER 5 SUMMARY OF CONCLUSION AND FUTURE RESEARCH

The delay calculations of DDI differ from isolated intersection on the delay calculation of internal lane, which is served with different inflows that come from off ramp left turn and arterial through movement. These flows can be served as saturated flow or just arrival rate, complicating the modeling part of the analysis and making it heavily dependent on the phasing sequence in place. With the introduced overlap and offset, different sequences are incorporated into a uniform structure to increase the accuracy of the delay modeling in DDI. The model uses the internal length, desired speed, saturated flow of each approach, all-red and amber time, arrival rate of each direction and timing plan as input variables. A series of intermediate variables are also introduced in the paper. By simply changing the input parameters, for example, saturated upstream flow rate, length of internal lane, amber and all red time and desired speed, all kinds of configurations of DDI can be involved into the introduced model in this study. The results show the calculation results fit output from VISSIM very well, with R-Square values of 0.9968 for the westbound internal lane, 0.9914 for eastbound internal lane, and 0.9949 for total delay of those two directions.

This paper arises the concern of safety issues for implementation of Ecodriving vehicles. However, instead of considering to avoid EV involving into traffic–collision related incident by adding constraint into ecodriving control algorithm, this paper opens the door for another horizon, which aims to identify the influence of EVs on the following normal drivers in safety aspect.

Generally, following the EV is safer than following NV, as the EV tend to decelerate in advance hence making deceleration smoother. But we noticed the normal driving vehicles in this experiments tend to decelerate aggressively near the intersection, since they already got so close to the intersection when the signal turned red. Moreover, as EV could follow the planned speed trajectory to avoid stopping at stoplights most of time, it further increase the safety of FNV following them by eliminating unnecessary stop-orientated deceleration. However, the EV will present abnormal behaviors from FNV' perspective, such as start decelerating further away from intersection when signals are still on green and accelerating too slowly. Those behaviors are inclined to cause potential risks which indicated by TTC. The experimental design conducted in this paper is innovative in that it is able to test both the car-following behaviors when an EV is decelerating and accelerating. Besides, in the simulator programming, trigger-based scenario designs make sure the drivers switch to another scenario with exactly the same starting position and ensure the car-following behavior present at the beginning. The more detailed conclusion are reached below:

1. Overall, Following an EV is safer than following a NV, the rate of critical seconds of FNV decreased by 30.29% and 7.84% if the initial signals are set to be red and green respectively. Besides, in the deceleration part when the initial signal is red, the critical seconds rate decreased by 6.36% if following an EV. In addition, in the acceleration part, the critical seconds lowered by 60.54% and 50.40% if following an EV when initial signal is red and green respectively.

2. During certain parts of the optimization horizon: the initial signal part 1 and the deceleration part when initial signal is green, as well as the initial acceleration part. EVs

cause more critical situations for FNV than NVs. The EVs increase the critical seconds by 708.33% and 710.00% when the initial signal is red and green respectively in initial signal part I. Following an EV results in 25.88% grow of critical seconds in deceleration part when initial signal is set to be green. Moreover, in the initial acceleration part, the critical seconds increased by 139.35%, 210.07% and 432.43% when set speed limit at 45mph, 40mph and 35mph respectively when following an EV.

3. Initial signal status shows significant influence on TTC of FNV when following an EV in initial signal part, as it increases the critical seconds by 67.01% when change the setting of initial signal from red to green. The effect remains strong enough to make it even significant for deceleration part and the whole optimization horizon, as it result in grows of the critical seconds by 27.51% and 25.49% respectively. Besides, speed limit impact the TTC of FNV following an EV in initial acceleration part and acceleration part significantly. In the initial acceleration part, compared to when set speed limit at 45mph, the critical seconds increased by 150.10% and 166.73% when speed limit are 40mph and 35 mph respectively. As for acceleration part, the increase rate become 133.33% and 146.43% respectively. This is result from the different average acceleration of EV in scenarios with different speed limit, as indicated by the significance value from ANOVA for initial acceleration part.

4. Two EV elements: acceleration and DistanceToStoplight, were found to have significant influence on TTC of FNV following an EV in deceleration part. In which the TTC of FNV decreased when EVs decelerate more and get closer to intersection. In addition, all these Three EV elements: acceleration, SpeedToLimit and DistanceTosStoplight of EV show significant impact on TTC of FNV in the initial

acceleration part.To be more specific, the TTC is decreasing as the decreasing acceleration rate of EVs, and when EV accelerate to get closer to stoplight. However, the adjusted R square of this model is only 0.207 which indicates that there may be some other influential elements have not been considered or they do not have linear correlation.

The results of the analysis can be used to guide future ecodriving design and simulation in safety aspect. The optimization horizon and the deceleration part particularly, should have enough length to avoid dramatic deceleration. Especially during the circumstance where the green initial signal is long while the red time after it is very short. As in these circumstances, the green initial signal has long influential duration and the impact will be strengthen by the decreasing speed of EVs. Besides, in the acceleration part, the critical circumstance are more likely to occur when EVs accelerate slowly to have higher speed and get closer to the intersection. Moreover, the minimal threshold for acceleration of EVs should be developed in order to avoid causing serious risks and blocking the intersections. In addition, for the simulation aim to examine the eco-driving efficiency, the varied TTC threshold should be adopted as it changes with initial signal status and speed limit of the road, acceleration and DistanceToStoplight of the EVs in deceleration part and acceleration DistanceToStoplight and SpeedToLimit in the initial acceleration part.

REFERENCE

[1] Davis, S.C., S.E. Williams, and R.G. Boundy, *Transportation Energy Data Book: Edition 35*. 2016.

[2] EPA, A., *Inventory of US greenhouse gas emissions and sinks: 1990-2009.* Environmental Protection Agency2012, 2017.

[3] Abuzo, A. and Y. Muromachi, *Fuel Economy of Ecodriving Programs.* Transportation Research Record: Journal of the Transportation Research Board, 2014. **2427**: p. 34-40.

[4] Martin, E., N. Chan, and S. Shaheen, *How Public Education on Ecodriving Can Reduce Both Fuel Use and Greenhouse Gas Emissions.* Transportation Research Record: Journal of the Transportation Research Board, 2012. **2287**: p. 163-173.

[5] Hu, J., et al., *Integrated optimal eco-driving on rolling terrain for hybrid electric vehicle with vehicle-infrastructure communication.* Transportation Research Part C: Emerging Technologies, 2016. **68**: p. 228-244.

[6] Chen, Z., et al., *Model for Optimization of Ecodriving at Signalized Intersections.* Transportation Research Record: Journal of the Transportation Research Board, 2014. **2427**: p. 54-62.

[7] Ahn, K. and H. Rakha, *Ecolane Applications.* Transportation Research Record: Journal of the Transportation Research Board, 2014. **2427**: p. 41-53.

[8] Xia, H., et al. *Field operational testing of eco-approach technology at a fixed-time signalized intersection*. in *Intelligent Transportation Systems (ITSC), 2012 15th International IEEE Conference on*. 2012. IEEE.

[9] Guan, T. and C.W. Frey. *Predictive fuel efficiency optimization using traffic light timings and fuel consumption model*. in *Intelligent Transportation Systems-(ITSC), 2013 16th International IEEE Conference on*. 2013. IEEE.

[10] De Nunzio, G., et al., *Eco‐driving in urban traffic networks using traffic signals information.* International Journal of Robust and Nonlinear Control, 2015.

[11] Xia, H., et al. *Development and evaluation of an enhanced eco-approach traffic signal application for connected vehicles*. in *Intelligent Transportation Systems-(ITSC), 2013 16th International IEEE Conference on*. 2013. IEEE.

[12] Kamal, M.A.S., et al., *Model predictive control of vehicles on urban roads for improved fuel economy.* IEEE Transactions on control systems technology, 2013. **21**(3): p. 831-841.

[13] Jin, Q., et al., *Power-Based Optimal Longitudinal Control for a Connected Eco-Driving System.* IEEE Transactions on Intelligent Transportation Systems, 2016. **17**(10): p. 2900-2910.

[14] Mensing, F., et al., *Trajectory optimization for eco-driving taking into account traffic constraints.* Transportation Research Part D: Transport and Environment, 2013. **18**: p. 55-61.

[15] Chen, W., et al., *Platoon-Based Speed Control Algorithm for Ecodriving at Signalized Intersection.* Transportation Research Record: Journal of the Transportation Research Board, 2015. **2489**: p. 29-38.

[16] Kamalanathsharma, R. and H. Rakha, *Agent-Based Simulation of Ecospeed-Controlled Vehicles at Signalized Intersections.* Transportation Research Record: Journal of the Transportation Research Board, 2014(2427): p. 1-12.

[17] Kamalanathsharma, R.K., H.A. Rakha, and H. Yang, *Networkwide Impacts of Vehicle Ecospeed Control in the Vicinity of Traffic Signalized Intersections.* Transportation Research Record: Journal of the Transportation Research Board, 2015(2503): p. 91-99.

[18] van Katwijk, R., et al. *Providing speed advice to vehicles approaching an intersection: evaluation and lessons learned*. in *Transportation Research Board 92nd Annual Meeting*. 2013.

[19] Jamson, A.H., D.L. Hibberd, and N. Merat, *Interface design considerations for an in-vehicle eco-driving assistance system.* Transportation Research Part C: Emerging Technologies, 2015. **58**: p. 642-656.

[20] Hallihan, G., et al., *Effects of Hybrid Interface on Ecodriving and Driver Distraction.* Transportation Research Record: Journal of the Transportation Research Board, 2011. **2248**: p. 74-80.

[21] Rakha, H.A., et al., *Virginia tech comprehensive power-based fuel consumption model: model development and testing.* Transportation Research Part D: Transport and Environment, 2011. **16**(7): p. 492-503.

[22] Saffarzadeh, M., et al. *A general formulation for time-to-collision safety indicator*. in *Proceedings of the Institution of Civil Engineers-Transport*. 2013. Thomas Telford Ltd.

[23] Machiani, S.G. and M. Abbas, *Safety surrogate histograms (SSH): A novel real-time safety assessment of dilemma zone related conflicts at signalized intersections.* Accident Analysis & Prevention, 2016. **96**: p. 361-370.

[24] Chlewicki, G., *Should the diverging diamond interchange always be considered a diamond interchange form?* Transportation Research Record: Journal of the Transportation Research Board, 2011(2223): p. 88-95.
[25] Hainen, A.M., et al., *Performance Measures for Optimizing Diverging Interchanges and Outcome Assessment with Drone Video.* Transportation Research Record: Journal of the Transportation Research Board, 2015(2487): p. 31-43.
[26] Xu, H., et al., *Control delay calculation at diverging diamond interchanges.* Transportation Research Record: Journal of the Transportation Research Board, 2011(2257): p. 121-130.